Synaptic Zn^{2+} potentiates the effects of cocaine on striatal dopamine neurotransmission and behavior

Juan L. Gomez[1], Jordi Bonaventura[1], Jacqueline Keighron[2], Kelsey M. Wright[1], Dondre L. Marable[1], Lionel A. Rodriguez[1], Sherry Lam[1], Meghan L. Carlton[1], Randall J. Ellis[1], Chloe Jordan[3], Guo-hua Bi[3], Oscar Solis[1], Marco Pignatelli[4], Michael J. Bannon[5], Zheng-Xiong Xi[3], Gianluigi Tanda[2], Michael Michaelides[1, 6*]

[1]Biobehavioral Imaging and Molecular Neuropsychopharmacology Unit, National Institute on Drug Abuse Intramural Research Program, Baltimore, MD, 21224, USA

[2]Medication Development Program, National Institute on Drug Abuse Intramural Research Program, Baltimore, MD, 21224, USA

[3]Addiction Biology Unit, National Institute on Drug Abuse Intramural Research Program, Baltimore, MD, 21224, USA

[4]Department of Psychiatry and Taylor Family Institute for Innovative Psychiatric Research, Washington University School of Medicine, St Louis, MO 63110, USA

[5]Department of Pharmacology, Wayne State University School of Medicine, Detroit, MI, 48201, USA

[6]Department of Psychiatry, Johns Hopkins School of Medicine, Baltimore, MD, 21205, USA

*Correspondence:

Michael Michaelides, PhD

251 Bayview Blvd, Room 05A721A

Baltimore, MD 21224

Tel: +1-443-740-2894

Fax: +1-443-740-2734

mike.michaelides@nih.gov

Abstract

Cocaine binds to the dopamine (DA) transporter (DAT) to regulate cocaine reward and seeking behavior. Zinc (Zn^{2+}) also binds to the DAT, but the *in vivo* relevance of this interaction is unknown. We found that Zn^{2+} concentrations in postmortem brain (caudate) tissue from humans who died of cocaine overdose were significantly lower than in control subjects. Moreover, the level of striatal Zn^{2+} content in these subjects negatively correlated with plasma levels of benzoylecgonine, a cocaine metabolite indicative of recent use. In mice, repeated cocaine exposure increased synaptic Zn^{2+} concentrations in the caudate putamen (CPu) and nucleus accumbens (NAc). Cocaine-induced increases in Zn^{2+} were dependent on the Zn^{2+} transporter 3 (ZnT3), a neuronal Zn^{2+} transporter localized to synaptic vesicle membranes, as ZnT3 knockout (KO) mice were insensitive to cocaine-induced increases in striatal Zn^{2+}. ZnT3 KO mice showed significantly lower electrically-evoked DA release and greater DA clearance when exposed to cocaine compared to controls. ZnT3 KO mice also displayed significant reductions in cocaine locomotor sensitization, conditioned place preference (CPP), self-administration, and reinstatement compared to control mice and were insensitive to cocaine-induced increases in striatal DAT binding. Finally, dietary Zn^{2+} deficiency in mice resulted in decreased striatal Zn^{2+} content, cocaine locomotor sensitization, CPP, and striatal DAT binding. These results indicate that cocaine increases synaptic Zn^{2+} release and turnover/metabolism in the striatum, and that synaptically-released Zn^{2+} potentiates the effects of cocaine on striatal DA neurotransmission and behavior and is required for cocaine-primed reinstatement. In sum, these findings reveal new insights into cocaine's pharmacological mechanism of action and suggest that Zn^{2+} may serve as an environmentally-derived regulator of DA neurotransmission, cocaine pharmacodynamics, and vulnerability to cocaine use disorders.

Introduction

Zinc (Zn^{2+}) is an essential trace element necessary for normal brain function (1-6). Within the brain it exists in two forms; a "fixed", protein-bound form, which serves as a catalytic co-factor or as a structural component to Zn^{2+} binding proteins, and comprises ~90% of total brain concentration, or a "free", or labile/chelatable form, comprising ~10% of total brain concentration. Labile Zn^{2+} is also referred to as "synaptic" Zn^{2+} as it is localized to synaptic vesicles in a subset of glutamatergic neurons, also referred to as "zincergic" neurons (7). Synaptic Zn^{2+} is found in several regions such as cortex (layers 2/3, 5 and 6), hippocampus, striatum, amygdala and is generally not present in thalamus (7, 8).

Synaptic Zn^{2+} levels are dependent on the Zn^{2+} transporter 3 (ZnT3) (9, 10), a neuronal-specific Zn^{2+} transporter localized to the membrane of synaptic vesicles. ZnT3 knockout (KO) mice lack the ability to package Zn^{2+} into these vesicles and consequently lack synaptic Zn^{2+} release (9, 10). ZnT3 KO mice are viable, fertile, and do not show major behavioral abnormalities across spatial learning, memory, or sensorimotor tasks, though they do exhibit small deficits in skilled reaching tasks (11, 12), fear learning (13), and sensory deficits (14, 15).

In terms of function, synaptic Zn^{2+} is released upon neuronal activation, serves as a key regulator of neurotransmitter signaling, and as such has also been referred to as a neurotransmitter (1-6). Tonic extracellular Zn^{2+} concentrations are estimated to be at <25 nM (16). However, upon physiological zincergic neuron activation and subsequent release, phasic Zn^{2+} concentrations can increase up to 10 μM (17). In this way, Zn^{2+} is thought to exert various effects on neurotransmission by binding to synaptic proteins that contain either low- or high-affinity Zn^{2+} binding sites (6). One such protein is the dopamine transporter (DAT), which contains four high-affinity Zn^{2+} binding sites on its extracellular domain (18-22).

Studies have shown that cocaine binds to the DAT to inhibit synaptic DA reuptake, which leads to an increase of extracellular DA (23). This mechanism underlies the direct subjective responses that accompany cocaine use (24), and is critical to cocaine self-administration in laboratory models, and cocaine reward and abuse liability in humans (25). *In vitro* assays have shown that when Zn^{2+} binds to the DAT it promotes a conformation that inhibits DA uptake and, when cocaine is present, Zn^{2+} can increase cocaine's affinity and can modulate its potency to inhibit DA uptake (18-22). Interestingly, synaptic Zn^{2+} is present in the striatum (26, 27) where the DAT is found in highest concentration (28), and synaptic Zn^{2+} depletion in this region improves

84 motor deficits and memory impairments caused by loss of striatal DAergic fibers (29). These prior
85 studies suggest that synaptic Zn^{2+} may modulate *in vivo* DAT function and cocaine-DAT
86 pharmacodynamic interactions in the striatum. However, the extent to which such interactions
87 occur is unclear.

88 In addition to ZnT3, synaptic Zn^{2+} levels also depend on the environmental availability of
89 Zn^{2+} which is obtained exclusively via the diet. Consequently, dietary factors which limit Zn^{2+}
90 intake influence both synaptic Zn^{2+} levels and ZnT3 expression (30, 31). In fact, as the body lacks
91 a specialized system for its storage, Zn^{2+} needs to be consumed continuously to avoid a state of
92 deficiency which itself can have profound changes in both the periphery as well as in brain function
93 (32). Human drug users generally do not follow a life-style that prioritizes nutritional needs and
94 are known to exhibit nutritional deficiencies including dysregulated blood and hair Zn^{2+} content
95 (33-38). However, whether such deficits are involved in the neurobiological changes associated
96 with cocaine use or use of other drugs is unknown.
97

98 **Methods**

99 Subjects

100 De-identified postmortem human brain specimens were collected during the routine
101 autopsy process as described in detail previously (39, 40). Briefly, the cause and manner of death
102 were determined by forensic pathologists following medico-legal investigations that evaluated the
103 circumstances of death including medical records, police reports, autopsy results, and toxicological
104 data. Inclusion in the cocaine cohort (n = 20; 10 Caucasian, 10 African-American) was based on
105 cocaine abuse as the cause of death, a documented history of drug abuse, and a toxicology positive
106 for high levels of the cocaine metabolite benzoylecgonine and, in most cases, the short-lived
107 cocaine adulterant levamisole, both indicative of recent cocaine use prior to death. Control subjects
108 (n=20; 10 Caucasian, 10 African-American) died as a result of cardiovascular disease or gunshot
109 wound, had no documented history of drug abuse, and tested negative for cocaine and other drugs
110 of abuse. Exclusion criteria for the study included a known history of neurological or psychiatric
111 illness, death by suicide, estimated postmortem interval exceeding 20 hr, evidence of
112 neuropathology (e.g. encephalitis, stroke), or chronic illness (e.g. cirrhosis, cancer, HIV, prolonged
113 hospitalization). The final groups did not differ with regard to age for race, nor with regard to brain

114 pH, a well-established measure of sample quality and perimortem agonal state (41). Tissue from
115 one cocaine user was not included due to very high cocaine metabolite levels.
116 Given that the human tissue samples available consisted only of males, and therefore all
117 human data were limited to this sex, we focused on male mice for all other mechanistic
118 experiments. Male C57Bl/6J mice were acquired from Jackson Labs at 8-weeks of age. Breeding
119 pairs of *Slc30a3* (ZnT3) knockout mice were obtained from Dr. Thanos Tzounopoulos at the
120 University of Pittsburgh and bred at the National Institute on Drug Abuse (NIDA) (Baltimore,
121 MD) on a C57Bl/6J background. Mice were genotyped by Transnetyx (Cordova, TN). All mice
122 were male and matched for age and weight. Mice were single-housed during experimental testing
123 in a temperature and humidity-controlled environment on a regular light cycle (on at 7 am and off
124 at 7 pm). Food and water were available ad libitum and mice were acclimated prior to any
125 behavioral procedures by handling. All experimental procedures were carried out in accordance
126 with the National Institutes of Health Guide for the Care and Use of Laboratory Animals and were
127 approved by the Animal Care and Use Committee of NIDA.
128
129 Total Reflection X-ray Spectroscopy (TXRF)
130 Tissue samples were collected and weighed in 1.5 mL Eppendorf tubes. The weight of the
131 tissue was directly used to calculate element concentrations in µg/kg units. Each tissue sample was
132 dissolved in 100 µL of nitric acid (Sigma: NX0408) with 2 µL of a gallium standard (conc. 1000
133 ppm). Each sample was assessed in duplicate for TXRF elemental analysis using an S2 Picofox
134 (Bruker, Billerica, MA). This instrument exposes the sample to an X-ray beam and measures
135 fluorescence radiation specific to the element(s) of interest. Human samples were prepared from
136 postmortem tissue collected from the anterior caudate. Wild-type (WT) or ZnT3 KO mice received
137 either saline, a single cocaine injection (20 mg/kg, i.p), or 8 repeated daily cocaine (20 mg/kg, i.p)
138 injections and were killed 24 hrs after the last injection. Mice fed the 30 ppm and 5 ppm Zn^{2+} diets
139 were exposed to each respective diet for 35 days and then killed. Mouse samples were prepared
140 by slicing flash frozen tissue on a cryostat (100 µm sections from Bregma 1.00 mm to 0.00 mm)
141 or dissecting the cortex and striatum from each section.
142
143 Synchrotron X-ray Fluorescence Microspectroscopy (µXRFS)

144 Brain concentrations and distributions of Zn^{2+} from C57BL/6J mice injected with saline or
145 cocaine (10 mg/kg, i.p.) every other day for 8 days and killed 24 hrs after the last injection were
146 measured at the X26a beamline at the National Synchrotron Light Source (NSLS) at Brookhaven
147 National Laboratory (Upton, NY). The synchrotron X-ray beam was tuned to 12 keV using a
148 Si(111) channel-cut monochromotor. The monochromatic beam was then collimated to 350
149 μm×350 μm and then focused to approximately 6 μm×10 μm using Rh-coated silicon mirrors in a
150 Kirkpatrick–Baez (KB) geometry. The sample was placed at a 45° angle to the incident X-ray
151 beam and X-ray fluorescence was detected with an energy dispersive, 9-element germanium array
152 detector (Canberra, Meriden, CT) oriented at 90° to the incident beam. The sample was
153 approximately 6 cm from the detector. A light microscope objective (Mitutoyo, M Plan Apo 5X)
154 was coupled to a digital CCD camera for sample viewing. Energy dispersive spectra were collected
155 by raster-scanning the sample through the X-ray beam using a dwell time of 0.3 s/pixel and a step
156 size of 10 μm. Zn Kα, fluorescence counts were then extracted from background-corrected energy
157 dispersive spectra. All data were normalized to variations in incident photon flux by normalizing
158 to changes in I0 measured by ion chamber upstream of the KB optics. XRFS calibration standards
159 on Nuclepore® polycarbonate aerosol membranes expressing known (±5%) concentrations of Zn
160 (48.4 $\mu g/cm^2$) were also imaged in parallel to the samples (Micromatter, Vancouver, BC) and used
161 to express results as $\mu g/cm^2$. Image analysis was carried out using ImageJ (National Institutes of
162 Health, Bethesda, MD). Regions of interest (ROI) were drawn onto the cortex (Ctx), caudate
163 putamen (CPu), nucleus accumbens (NAc), and measurements for each ROI were obtained.

164

165 <u>Zinc-Selenium Autometallography ($ZnSe^{AMG}$)</u>

166 WT and ZnT3 KO mice were anesthetized with a ketamine-xylazine cocktail
167 (ket=60mg/kg + xyl=12mg/kg) and injected (i.p.) with 15 mg/kg sodium selenite (Sigma Aldrich:
168 214485) and placed on a heating pad while anesthetized for 60 minutes. Mice were then perfused
169 with 0.1M phosphate buffer for 5 minutes. Brain tissue was dissected, and flash frozen in dry ice
170 cooled isopentane and stored at -80ºC until sectioning. Coronal brain sections (20 μm) were thaw
171 mounted at the level of the striatum and hippocampus on positively-charged glass slides. Slides
172 were stored at -20ºC until staining. Slides were loaded in non-metallic staining racks and allowed
173 to reach room temperature. Slides were fixed in 95% ethanol for 15 min followed by hydration in
174 70% (2 min) and 50% (2 min) ethanol ending in 3 x 2 min distilled water rinses. Slides were dipped

175 in 0.5% gelatin and air dried prior to physical development. Developer was made by mixing Gum
176 Arabic (50% solution, 100mL), citrate buffer (2.0M, 20mL), hydroquinone (1.7g in 30mL
177 DDH_2O), silver lactate (0.22g in 30mL H_20), and DDH_2O (200mL). Developer was poured onto
178 slides, incubated for 60 min in the dark then quickly checked at 10 min intervals until sections are
179 dark brown. Slides were washed in slowly flowing tap water (37ºC) for 10 min to remove gelatin
180 then rinsed 3 x 2 min in distilled water. Slides were then incubated in 5% sodium thiosulphate
181 (12min) and rinsed 2 x 2min in distilled water and post-fixed in 70% ethanol (30min). Optional
182 counter stain using cresyl violet or toluidine blue (5min) followed by rinse 4 x 30 sec rinse in
183 distilled water. Finally, slides were dehydrated in 95% ethanol (5min), 100% ethanol 2 x 5 min,
184 xylene 2 x 5 min, and coverslipped with permount. Stained sections were imaged using brightfield
185 microscopy.
186
187 ^{65}Zn Uptake Experiments using Positron Emission Tomography (PET)
188 WT and ZnT3 KO mice were anesthetized with isoflurane and placed in a prone position
189 on the scanner bed of a nanoScan PET/CT (Mediso, USA) injected intravenously (~150 µL) with
190 $^{65}ZnCl_2$ (~2.2 MBq) and PET data were acquired for 2 hours followed by a CT scan. After
191 scanning, animals were returned to their home cage. Scans were repeated on days 1, 3, 7, and 14.
192 For cocaine experiments, C57Bl/6J mice were injected with $^{65}ZnCl_2$ as above and then injected
193 immediately with saline or cocaine (20 mg/kg, i.p). Saline and cocaine injections continued daily
194 for 7 days. Mice were scanned on Day 1 and Day 7 after $^{65}ZnCl_2$ injection as above. In all cases,
195 the PET data were reconstructed and corrected for dead-time and radioactive decay. Qualitative
196 and quantitative assessments of PET images were performed using the PMOD software
197 environment (PMOD Technologies, Zurich Switzerland). Time-activity curves were generated
198 using manually drawn volumes of interest using the CT image as a reference. Standardized uptake
199 values (SUV) were calculated using the formula $SUV(i) = C(i) / (ID \times BW)$ where C(i) is the
200 activity value at a given time point (in kBq/cc), ID is the injected dose (in MBq) and BW is the
201 animal's body weight (in kg). For voxel-wise analyses we used Statistical Parametric Mapping
202 (SPM12, London, UK) as previously described (42). First, all the images were co-registered and
203 masked to the reference mouse atlas in PMOD. Regional changes in uptake were assessed relative
204 to global (whole-brain) uptake. For the cocaine experiments, a repeated measures analysis of
205 variance (ANOVA) model was used that defined saline vs. cocaine-treated mice scanned at 1- and

206 7-days post $^{65}ZnCl_2$ injection. Images were subtracted after intensity normalization to 100 by the
207 proportional scaling method. After estimation of the statistical model, a contrast (Cocaine >
208 Vehicle) was applied to reveal the effects of interest. These effects were overlaid on the reference
209 MRI. An uncorrected *P*-value of 0.05 with a cluster threshold value of 50 were used as thresholds
210 to determine statistical significance.
211
212 *Ex vivo* ^{65}Zn autoradiography
213 One day after the last PET scan, WT and ZnT3 KO mice were killed and brain tissue was
214 dissected, flash frozen in isopentane, and stored at -80ºC until sectioning. Tissue was sectioned
215 and thaw mounted on positively charged glass slides. Slides were placed on BAS-IP SR 2040 E
216 Super Resolution phosphor screens (GE Healthcare) for 14-days and imaged using a phosphor
217 imager (Typhoon FLA 7000; GE Healthcare).
218
219 Radioligand Binding Assays
220 Brains from killed C57Bl/6J mice were removed and striata dissected and quickly frozen
221 until use. The tissue was weighed and suspended in 10 times (w/v) of ice-cold Tris-HCl buffer (50
222 mM, pH 7.4). The suspension was homogenized with a Polytron homogenizer (Kinematica, Basel,
223 Switzerland) under ice. Homogenates were centrifuged at 48,000g (50 min, 4 °C) and washed
224 twice in the same conditions to isolate the membrane fraction. Protein was quantified by the
225 bicinchoninic acid method (Pierce). For competition experiments, membrane suspensions (50 µg
226 of protein/ml) were incubated in 50 mM Tris-HCl (pH 7.4) 0.5 nM of [^{3H}]WIN-35428 (Perkin-
227 Elmer) and increasing concentrations of the indicated competing drugs (WIN-35428 or cocaine)
228 in the presence or the absence of 100 nM, 10 µM or 1 mM of $ZnCl_2$ during 2 h at RT. Nonspecific
229 binding was determined in the presence of 100 µM cocaine. In all cases, free and membrane-bound
230 radioligand were separated by rapid filtration through Whatman (Clifton, NJ) GF/B filters, pre-
231 soaked in 0.05% polyethyleneimine by using a Brandel R48 filtering manifold (Brandel Inc.,
232 Gaithersburg, MD). The filters were washed twice with 5 ml of cold buffer and transferred to
233 scintillation vials. Beckman Ready Safe scintillation cocktail (3.0 ml) was added, and the vials
234 were counted the next day with a Beckman 6000 liquid scintillation counter (Beckman Coulter
235 Instruments, Fullerton, CA) at 50% efficiency.
236

237 *In vitro* Autoradiography using [^{3}H]WIN-35,428

238 Brain tissue from WT and ZnT3 KO mice was dissected, flash frozen in isopentane, and
239 stored at -80ºC until sectioning. Tissue was sliced on a cryostat at 16 µm and thaw mounted on
240 positively charged glass slides and stored at -20ºC until autoradiography. Incubation Buffer
241 consisted of 50 mM Tris-HCl (7.4 pH) and 100 mM NaCl in deionized water. [^{3}H]WIN-35,428
242 Total binding buffer (S.A. 82.9 Ci/mmol, Conc. 1 mCi/mL) was made in incubation buffer at a
243 concentration of 10 nM. $ZnCl_2$ binding buffer was made using the Total binding buffer stock and
244 adding $ZnCl_2$ for a concentration of 10 µM. Slides were pre-incubated in ice-cold incubation buffer
245 for 20 minutes then transferred to respective radioactive incubation buffers (i.e. total or
246 total+$ZnCl_2$) for 120 minutes on ice. Slides were then washed 2 x 1min in ice-cold 50 mM Tris-
247 HCl (pH=7.4) then dipped (30 sec) in ice-cold deionized water. Slides were dried under stream of
248 cool air and placed on BAS-IP TR 2025 E Tritium Screen (GE Healthcare) for 5-days and imaged
249 using a phosphor imager (Typhoon FLA 7000; GE Healthcare). Sections were analyzed using
250 Multigauge software (Fujifilm, Japan).

251

252 *In vivo* Fast Scan Cyclic Voltammetry (FSCV)

253 FSCV procedures follow those of recently published work from our laboratory in
254 anesthetized mice using electrical stimulation (43). Briefly, glass sealed 100 µm carbon fiber
255 microelectrodes were pre-calibrated with known concentrations of dopamine and changes in pH
256 to allow for a principal component analysis (PCA) of the raw data using HDCV (UNC, Chapel
257 Hill, NC). Dopamine was identified by cyclic voltammogram using a voltage scan from -0.3 to
258 1.4V at 400 V/s. During the experiment an external stimulus was applied using the tungsten
259 electrode every 5 min comprised of 24 pulses 4ms in width at 60 Hz and 180 µA while the working
260 electrode was implanted in the striatum (AP: +1.5 mm; ML: ±1.0 mm; DV: -3.2 to -3.7 mm from
261 bregma). After PCA data were analyzed to determine the DA_{Max} and DA clearance rate using a
262 custom macro written in Igor Carbon Pro which identified peaks greater than 3x root mean square
263 noise and fit to equation 1 where DA_{Max} represents the peak DA concentration measured, k is the
264 rate constant, and t is time (43).

265 (1) $DA(t) = DA_{Max}e^{-k(t-t_0)}$

266

267 Cocaine Locomotor Sensitization

Each session during the development phase was 30 minutes and mice were only exposed to one session per day with locomotor activity quantified as distance traveled (cm). All injections were administered (i.p.). Mice were first habituated to the locomotor activity chambers (Opto-varimex ATM3, Columbus Instruments). On the next two sessions mice were injected with saline and placed in the chambers. On the following five sessions, separate groups were injected with either saline or cocaine (10 mg/kg) in a counterbalanced design. Mice were then allowed 7-days of withdrawal in the colony room and then returned to the behavior room for testing expression of sensitization. Briefly, all mice were allowed access to the activity chambers for 60 minutes followed by increasing doses of cocaine (saline, 5, 10, 20 mg/kg) every 60 minutes. Data collection was paused but chambers were not cleaned in-between cocaine dosing, each mouse was picked up, injected, and placed back in chamber to continue data collection.

Cocaine Conditioned Place Preference (CPP)

The task consisted of 10 sessions, 1 per day, in chambers with two visually distinct sides, one with clear walls and white floor and one with checkered walls and black floor. The sides were divided by a door with and without access to the other side. Locomotor activity was measured by way of time spent in each chamber as well as total distance traveled (Opto-varimex ATM3, Columbus Instruments). In the first session the mice could explore both sides of a conditioning box for 15 minutes to determine inherent side preference, designated as the Pre-Test. Using this data, the cocaine-paired side was pseudo-randomized so that mice with a preference for one side (>60%) were cocaine-paired on the other, non-preferred side. Mice with no side preference were cocaine-paired in a counterbalanced fashion. Separate groups of mice were conditioned with either a 5, 10, or 20 mg/kg dose of cocaine. In an alternating fashion for 8-days, mice were injected (i.p.) with either saline or cocaine and placed in the predetermined drug/no drug side of the chamber for 30 minutes. The mice had no physical access to the other side but were still able to see through the clear divider wall. Each mouse had a total of 4 saline-paired days and 4 cocaine-paired days. The last session was the same as the first and designated the Test session. Time spent in the cocaine-paired chamber during the Pre-Test session (prior to conditioning) was subtracted from time spent in the cocaine-paired chamber during the Test session and expressed as the Preference score.

Mouse Intravenous Cocaine Self-Administration

299 Mice were implanted with jugular vein catheters under ketamine/xylazine anesthesia and
300 using aseptic surgical techniques. A 6.0 cm length MicroRenathane (ID 0.012″, OD 0.025″;
301 Braintree Scientific Inc., Braintree, MA, USA) catheter was inserted 1.2 cm into the right jugular
302 vein and anchored to a 24-gauge steel cannula (Plastics One, Roanoke, VA, USA) that was bent
303 at a 100° angle and mounted to the skull with cyanoacrylate glue and dental acrylic. A 2.5-cm
304 extension of flexible tubing was connected to the distal end of the cannula. The mice were allowed
305 5–7 days for recovery, during which time 0.05 ml of a 0.9% saline solution containing 20 IU/ml
306 heparin and 0.33 mg/ml gentamycin was infused daily through the catheter to prevent catheter
307 clotting and infection. Thereafter, 0.05 ml of 0.9% saline solution containing 20 IU/ml heparin was
308 infused immediately prior to and immediately following each daily self-administration session.
309 When needed, i.v. brevital (a barbiturate) was used to test catheter patency between the self-
310 administration sessions. During cocaine self-administration sessions, the flexible tubing extension
311 was connected to a perfusion pump (Med Associates, Fairfax, VT) via a PE50 tubing connector.
312 After daily self-administration sessions, the free end of the cannula guide was always kept sealed.
313 Operant test chambers (Med Associates, Fairfax, VT) contained two levers (active and
314 inactive) located 2.5 cm above the floor as well as a cue light above each lever. A house light
315 mounted on the opposite side of the chamber signaled the start of each 3 hr session and remained
316 illuminated until the session ended. For self-administration sessions, a liquid swivel mounted on a
317 balance arm above the chamber allowed for i.v. drug delivery in freely-moving mice. Depression
318 of the active lever resulted in the activation of an infusion pump; depression of the inactive lever
319 was recorded but had no scheduled consequences. Each infusion was paired with two discrete cues:
320 illumination of the cue light above the active lever, and a cue tone that lasted for the duration of
321 the infusion. Experimental events were controlled by a PC programmed in Medstate Notation and
322 connected to a Med Associates interface.
323 After recovery from surgery, mice were placed into operant chambers and allowed to lever-
324 press for i.v. cocaine self-administration under a fixed-ratio 1 (FR1) reinforcement schedule (i.e.,
325 each lever press leads to one cocaine infusion) for 3 h daily. Each cocaine infusion lasted 4.2 sec,
326 during which additional active lever responses were recorded but had no consequences (i.e., non-
327 reinforced active lever response). Mice were trained initially for a high unit dose of cocaine
328 (1 mg/kg/infusion) to potentiate acquisition of self-administration until stable self-administration
329 was achieved, which was defined as earning at least 20 infusions per 3 hr session and an

active/inactive lever press ratio exceeding 2:1. Then the mice were switched to a multiple-dose schedule to observe the dose-dependent cocaine self-administration according to a descending cocaine dose sequence from the initial dose of 1 mg/kg/infusion (sessions 1-13) to 0.5 mg/kg/infusion (sessions 14-20), 0.25 mg/kg/infusion (sessions 21-23), 0.125 mg/kg/infusion (sessions 24-27), and 0.0625 mg/kg/infusion (sessions 28-29). Mice that did not reach stability criteria, lost catheter patency, or showed excessive high-level inactive lever responding (>100 presses per session) were excluded from further experimentation. To prevent cocaine overdose, maximally allowed cocaine infusions were 50 (0.1 and 0.5 mg/kg/infusion), 100 (0.25 mg/kg/infusion), 200 (0.125 mg/kg/infusion), or 400 (0.0625 mg/kg/infusion), respectively during each 3-h session. The number of cocaine infusions earned, and active and inactive lever responses were recorded for each session. The last 2-3 days of cocaine self-administration data at each dose were averaged and used to compare dose-response performance between WT and KO mice.

After the completion of the above cocaine dose-response experiment, the animals were switched to cocaine self-administration under PR reinforcement schedule. During PR conditions, the work requirement (lever presses) needed to receive a cocaine infusion was raised progressively within each test session according to the following PR series: 1, 2, 4, 6, 9, 12, 15, 20, 25, 32, 40, 50, 62, 77, 95, 118, 145, 178, 219, 268, 328, 402, 492, and 603 until the break point was reached. The break point was defined as the maximal workload (i.e., number of lever presses) completed for the last cocaine infusion prior to a 1-h period during which no infusions were obtained by the animal. Animals were tested for cocaine self-administration under PR reinforcement at three doses (starting at 0.25, then 1 and then 0.5 mg/kg/infusion) from days 30 to 38.

After the completion of the PR experiments, the same groups of animals continued for cocaine extinction and reinstatement tests. During extinction, syringe pumps were turned off and the cocaine-associated cue light and tone were unavailable. Thus, lever pressing was recorded but had no scheduled consequences. Extinction training continued for about 20 days until the extinction criteria were met (i.e., lever responding <20% of the self-administration baseline) for at least 3 sessions. Mice then received a 10 mg/kg i.p cocaine injection to evoke reinstatement of drug-seeking behavior. During reinstatement testing, active lever presses lead to re-exposure to the cue light and tone previously paired with cocaine infusions, but not to actual cocaine infusions. Active and inactive lever responses were recorded for each extinction and reinstatement session.

360 Lever pressing behavior during the cocaine-primed session was compared to the average lever
361 pressies during the last 3 days of extinction.
362
363 Custom Diets
364 Diets were formulated by Research Diets, Inc via use of AIN-93M mature rodent diet. The
365 diets were compositionally identical, but one diet had an adequate amount of Zn^{2+} (30 ppm) and
366 the other diet had a deficient amount of Zn^{2+} (5 ppm). Zn^{2+} concentration in each diet was
367 confirmed in-house via random sampling of chow pellets and TXRF (S2 Picofox, Bruker,
368 Billerica, MA).
369
370 Body Weight and Food Intake Measurements
371 C56BL/6J mice arrived at the NIDA mouse colony and were allowed one week of
372 environmental acclimation with regular chow and water available *ad lib*. After the acclimation
373 period, mice were given a diet containing either 30 ppm Zn^{2+} or 5 ppm Zn^{2+} for a minimum of 35
374 days prior to any behavioral manipulations. Mice stayed on the diet until the completion of the
375 experiment. Mice were individually housed and weighed 3 times per week (MWF) along with food
376 weight to track the amount of food consumed.
377
378 Immunohistochemistry
379 Coronal sections were sliced on a cryostat (30 µm), collected in 6-well plates with PBS,
380 and stored at 4ºC until use. Sections were transferred to 12-well plates and permeabilized in
381 washing buffer (PBS + Triton X-100 0.1%) for 10 min at room temperature on shaker. Tissue was
382 blocked in blocking buffer (BSA 3% + PBS + Triton X-100 0.1%) for 60 min at RT on shaker.
383 Tissue was incubated overnight in primary ZnT3 antibody (1:500) (anti-rabbit, #197 003, Synaptic
384 Systems, Goettingen, Germany) at 4ºC. Tissue was washed with washing buffer 3 x 10 min at RT
385 then incubated in secondary antibody (Alexa 488-Rabbit #A1134, Thermo Fisher (1:400), Topro
386 (1:1200), and DAPI (1:600) for 2 hrs at RT in the dark. Tissue was washed with washing buffer 3
387 x 10 min, transferred to dish with PBS, mounted on positively charged glass slides, and
388 coverslipped with aqueous mounting medium (90% glycerol + 30 mM Tris-HCl, pH 8.0) and
389 imaged using confocal microscopy.
390

391 Statistics

392 Sample sizes were estimated based on prior experience with the specific
393 assays/experiments and expected effect sizes. Mice (with the exception of ZnT3 KO) were
394 randomly selected from littermates into experimental groups. Experiments were performed
395 unblinded. Depending on experiment, we used linear regression, unpaired t-tests, one sample non-
396 parametric (Wilcoxon) tests, one or two-way ANOVA or a mixed effects model (to account for
397 missing data) taking repeated measures (RM) into account when appropriate. Significant main or
398 interaction effects were followed by Holm-Sidak pairwise comparisons. All statistical tests were
399 evaluated at the $p \leq 0.05$ level. Estimations statistics were used for experiments with low sample
400 size (e.g. $n<5$) or with data that were not normally distributed (www.estimationstats.com)(44).

401

402 **Results**

403

404 **Striatal Zn^{2+} is low in human cocaine users and correlates with cocaine intake**

405 The highest DAT density in the brain is found in the striatum (28), a region heavily
406 implicated in cocaine addiction (45-48). Human drug users are characterized by nutritional
407 deficiencies and dysregulated blood and hair Zn^{2+} content (33-38) but whether they show deficits
408 in striatal Zn^{2+} is unknown. To assess this, we performed elemental profiling using total reflection
409 X-ray fluorescence spectroscopy (TXRF) in postmortem striatal tissue derived from humans
410 whose primary cause of death was attributed to cocaine abuse (n=19) or matched controls (n=20)
411 (Figure 1A). Cocaine users and controls did not differ in age (Figure 1B) or brain pH content
412 (Figure 1C). We found that cocaine users had significantly lower (unpaired t-test, $t=2.87$; $p=0.006$)
413 striatal Zn^{2+} levels compared to controls (Figure 1D). This difference was selective to Zn^{2+} as we
414 did not detect significant differences in other elements (Figure S1). Striatal Zn^{2+} levels in these
415 subjects significantly and negatively correlated (linear regression; $F(1, 17)=4.5$; $p=0.04$) with
416 plasma concentrations of benzoylecgonine, (Figure 1E) a stable cocaine metabolite indicative of
417 recent cocaine use (49).

418

419 **Cocaine increases synaptic Zn^{2+} release and uptake in the striatum**

420 To obtain mechanistic insights in the relationship between cocaine exposure and striatal
421 Zn^{2+} levels, we examined striatal Zn^{2+} content in mice exposed to cocaine. Unlike TXRF,

synchrotron X-ray fluorescence microspectroscopy (μSXRF) allows visualization and quantification of Zn^{2+} in brain slices (50, 51). We first verified that the distribution of Zn^{2+}, as detected by μSXRF in the hippocampus, where synaptic Zn^{2+} levels are high, coincided with distributions of ZnT3 immunolabeling and histochemically-reactive synaptic Zn^{2+} (52) (Figure S2). We then performed μSXRF in striatal sections from mice exposed to daily cocaine injections (10 mg/kg, intraperitoneal (IP), 4 days, n=4) and killed 24 hours later. We found that cocaine-exposed mice had significantly greater total Zn^{2+} levels in the caudate putamen (CPu) [unpaired mean difference: Veh vs. Coc=111; (95.0% CI 66.4, 139), p=0.003] and in the nucleus accumbens (NAc) [unpaired mean difference: Veh vs. Coc=65.3; (95.0% CI 47.4, 98.2); p<0.001] compared to vehicle-injected mice (n=5) (Figure 2, A and B). There was no significant difference in cortex [unpaired mean difference: Veh vs. Coc=77.8; (95.0% CI 85.1, 141); p=0.09].

ZnT3 KO mice lack the ability to package Zn^{2+} into synaptic vesicles and by extension cannot release synaptic Zn^{2+} (10). We hypothesized that the increase in cocaine-induced striatal Zn^{2+} we observed in mice was mediated via ZnT3. To assess this, we first confirmed that ZnT3 KO mice lack histochemically-reactive (52) synaptic Zn^{2+}. In agreement with prior findings (53), we found that synaptic Zn^{2+} was enriched in discrete areas including medial cortical regions, dorsomedial CPu, and medial NAc in wild-type (WT) mice (Figure 2C) and as expected, ZnT3 KO mice completely lacked synaptic Zn^{2+} (Figure 2D). We then exposed WT and ZnT3 KO mice to daily vehicle (n=6 WT, n=9 KO), a single (20 mg/kg/day, IP) cocaine injection (SC) (n=4 WT, n=4 KO) or repeated cocaine (RC) (20 mg/kg/day for 8 days, IP) (n=5 WT, n=4 KO) injections and killed them 24 hours later followed by dissection of medial frontal cortex and striatum and assessment of Zn^{2+} using TXRF. Vehicle-treated ZnT3 KO mice had significantly lower Zn^{2+} than vehicle-treated WT mice in cortex (Figure S3), where ZnT3 expression and synaptic Zn^{2+} pools are high (Figure 2C). In contrast, vehicle-treated WT and ZnT3 KO mice did not differ in striatal Zn^{2+}, as synaptic Zn^{2+} levels in this region are low (Figure 2, E and F) and differences under these basal circumstances were below the detection limit of TXRF (Figure 2E). WT mice exposed to a SC injection did not differ in striatal Zn^{2+} compared to vehicle-treated WT mice [shared control (WT VEH) comparison; unpaired mean difference: vehicle vs. SC=1.52; (95.0% CI -0.31, 2.84), p=0.07] (Figure 2, E and F). In agreement with results from our μSXRF experiments (Figure 2, A and B), WT mice exposed to RC injections had significantly greater striatal Zn^{2+} content than vehicle-treated WT mice [unpaired mean difference: vehicle vs. RC=3.41; (95.0% CI 0.76, 6.87),

453 p=0.03] (Figure 2, E and F). In contrast, cocaine exposure did not lead to any differences in striatal
454 Zn^{2+} in ZnT3 KO mice (Figure 2, E and F).

455 As a trace element, Zn^{2+} is challenging to study *in vivo*. Consequently, *in vivo* brain Zn^{2+}
456 kinetics have not been previously described. However, *ex vivo* studies using radioactive $^{65}ZnCl_2$
457 have shown that Zn^{2+} has unique brain kinetics, uptake, and biodistribution profiles. Specifically,
458 systemic injection of $^{65}ZnCl_2$ takes about 6 days to reach maximal brain uptake (54). Similarly,
459 another study estimated Zn^{2+} turnover in the brain to be a slow process, taking ~7 days (55).
460 Importantly, the *ex vivo* brain distribution of systemically-administered $^{65}ZnCl_2$ is dependent on
461 neuronal activity (56) and overlaps with both distribution of ZnT3 protein and histochemically-
462 reactive Zn^{2+} (54), suggesting that the majority of Zn^{2+} uptake to the brain is in the form of synaptic
463 Zn^{2+}. In agreement with this, studies have shown that $^{65}ZnCl_2$ is transported throughout the brain
464 in a trans-synaptic manner (57). Finally, like synaptic Zn^{2+} (31), $^{65}ZnCl_2$ brain uptake is dependent
465 on dietary Zn^{2+} intake (58). Collectively, these studies indicate that $^{65}ZnCl_2$ brain uptake can be
466 used as a measure of synaptic Zn^{2+} turnover/metabolism. Interestingly, ^{65}Zn produces annihilation
467 photons at 511 keV at a low (~3%) abundance and has a physical half-life of ~244 days. We
468 reasoned that these physical characteristics would be sufficient for noninvasive and longitudinal
469 measurements of $^{65}ZnCl_2$ uptake and kinetics using positron emission tomography (PET) and thus
470 could provide *in vivo* assessments of brain Zn^{2+} turnover/metabolism. To confirm, WT (n=2) and
471 ZnT3 KO (n=2) mice were injected intravenously (IV) with 2 μCi/g $^{65}ZnCl_2$ and scanned using
472 PET. Owing to the slow kinetics and long biological and physical half-lives of Zn^{2+} (54), mice
473 were scanned longitudinally at different days after $^{65}ZnCl_2$ injection (Figure 2G). ^{65}Zn showed
474 rapid brain uptake, exhibited slow brain clearance, and was detected in the brain up to 14 days
475 after injection (Figure 2, G and H and Figure S4). ZnT3 KO mice had lower brain uptake of $^{65}ZnCl_2$
476 at 7- and 14-days post injection compared to WT mice (Figure 2H). This was confirmed *ex vivo*
477 using autoradiography, which showed that ^{65}Zn brain distribution overlapped with distribution of
478 synaptic Zn^{2+} and ZnT3 protein in WT mice (Figure 2I and Figure S5). Notably, whereas ZnT3
479 KO mice did show some minimal $^{65}ZnCl_2$ uptake, perhaps representing non-specific uptake or a
480 result of other zinc transporters expressed in the brain (59), the distribution of $^{65}ZnCl_2$ uptake in
481 KO mice was largely absent from ZnT3-rich regions, indicating that it did not represent the
482 synaptic Zn^{2+} pool. Next, to examine effects of cocaine on $^{65}ZnCl_2$ brain uptake, we injected mice
483 with $^{65}ZnCl_2$ as above followed by daily vehicle (n=4) or cocaine (n=3) injections (20 mg/kg/day,

484 IP, 8 days) and performed PET. Compared to vehicle, cocaine significantly (1-way anova,
485 treatment main effect, t contrast (1, 4)=2.13; p=0.049) increased uptake of $^{65}ZnCl_2$ in brain regions
486 with high ZnT3 and synaptic Zn^{2+} levels, including the prelimbic, cingulate, sensory cortices, NAc,
487 hippocampus, and amygdala but decreased it in areas of low ZnT3 and synaptic Zn^{2+} levels like
488 thalamus (Figure 2J).
489
490
491 **Synaptic Zn^{2+} release increases the *in vivo* potency of cocaine on striatal DA**
492 **neurotransmission**
493 *In vitro* studies indicate that Zn^{2+} binds to the DAT and causes i) DA reuptake inhibition
494 and ii) increased cocaine DAT binding (18, 21, 22, 60, 61). We reproduced these findings using
495 mouse striatal membranes (n=6 mice/pooled) whereby a physiologically achievable concentration
496 (10 μM) of Zn^{2+} (1) significantly increased [unpaired mean difference: 0 vs. 10 μM =-0.627;
497 (95.0% CI -0.86, -0.41), p<0.001] cocaine binding and affinity to the DAT (Figure 3, A and B,
498 Figure S6). A higher, supraphysiological concentration (1 mM), decreased [unpaired mean
499 difference: 0 vs. 1000 μM =2.51; (95.0% CI 0.88, 3.43), p=0.06] cocaine affinity (Figure 3, A and
500 B). In agreement with the above results, 10 μM Zn^{2+} also significantly increased binding of
501 [^{3}H]WIN35,428 to the DAT in tissue sections (n=4 mice) (unpaired t-test, t=4.03; p=0.007) (Figure
502 3C).
503 To assess cocaine's *in vivo* effects at the DAT as a function of synaptic Zn^{2+}, we performed
504 *in vivo* fast scan cyclic voltammetry (FSCV) in the striatum of WT (n=4) and ZnT3 KO (n=4)
505 mice. Electrical stimulation of the medial forebrain bundle (MFB) was used to evoke DA release
506 in the striatum followed by escalating cocaine injections (5, 10, 20 mg/kg, IP) (Figure 3D). WT
507 and ZnT3 KO mice did not differ in baseline DA release or clearance (Figure S7). <u>DA release:</u>
508 Compared to Vehicle, we found that 5, 10, and 20 mg/kg cocaine significantly increased
509 electrically-evoked extracellular DA release in WT mice, but ZnT3 KO mice only showed a
510 significant increase at 20 mg/kg cocaine (Figure S7). ZnT3 KO mice also showed significantly
511 lower electrically-evoked extracellular DA release compared to WT mice (2-way RM anova;
512 genotype x time interaction, F(19, 114)=5.46; p<0.001) (Figure 3E, G). <u>DA clearance:</u> Compared
513 to Vehicle, 5, 10, and 20 mg/kg cocaine significantly decreased DA clearance in WT mice as
514 compared to Vehicle, but ZnT3 KO mice only showed significantly lower DA clearance at 20
515 mg/kg cocaine (Figure S7). ZnT3 KO mice showed significantly greater DA clearance in response

516 to cocaine compared to WT mice (2-way RM anova; genotype x time interaction, F(19, 114)=2.35
517 p=0.0029) (Figure 3F, H).
518
519 **Synaptic Zn^{2+} release potentiates cocaine locomotor sensitization, reward, seeking and is**
520 **required for cocaine-induced increases in DAT**
521 We hypothesized that cocaine-induced synaptic Zn^{2+} release would modulate cocaine-
522 related behavior. To examine this, we first tested ZnT3 KO mice for development and expression
523 of cocaine-induced locomotor sensitization. WT (n=15) and ZnT3 KO mice (n=16) both developed
524 locomotor sensitization to daily injections of cocaine (10 mg/kg/day, IP, 5 days) (2-way RM anova
525 with Holm-Sidak multiple comparisons, genotype x session interaction, F(3, 59)=7.07; p=0.004)
526 (Figure 4A). However, ZnT3 KO mice (n=16) showed significantly lower locomotor activity
527 compared to cocaine-treated WT mice on Day 1 (t=3.09; p=0.01) and Day 5 (t=3.22; p=0.009) of
528 the procedure. As expected, WT mice injected with cocaine showed significantly greater
529 locomotor activity than vehicle-treated WT (n=16) mice on Day 1 (t=5.54; p<0.001) and Day 5
530 (t=8.71; p<0.001). KO mice injected with cocaine showed significantly greater locomotor activity
531 than vehicle-treated KO (n=16) mice on Day 5 (t=5.68; p<0.001) but not on Day 1 (t=2.48;
532 p=0.08). One week later, vehicle-treated and cocaine-treated mice were tested for expression of
533 cocaine locomotor sensitization via exposure to escalating cocaine injections (5, 10, and 20 mg/kg,
534 IP). WT mice with prior cocaine exposure (cocaine-treated) (n=9) showed significantly greater (2-
535 way RM anova with Holm-Sidak multiple comparisons, genotype x time interaction, F(79,
536 1343)=1.85; p<0.001) expression of cocaine locomotor sensitization at 5 (66 min; t=3.65; p=0.02,
537 69 min; t=3.72; p=0.01) and 10 mg/kg cocaine (123 min; t=5.24; p<0.001, 126 min; t=6.03;
538 p<0.001, 129 min; t=5.19; p<0.001, 132 min; t=3.75; p=0.01, 135 min; t=3.54; p=0.03) compared
539 to vehicle-treated wild-type mice (n=10) (Figure 4B). In contrast, cocaine-treated KO mice (n=10)
540 did not show a significant increase in locomotor activity (2-way RM anova, genotype x time
541 interaction, F(79, 1422)=0.9197; p=0.67) compared to vehicle-treated KO mice (n=10) (Figure
542 4C). Neither WT nor ZnT3 KO cocaine-treated mice differed from the corresponding vehicle-
543 treated mice at a 20 mg/kg dose of cocaine (Figure 4, B and C).
544 Cocaine exposure increases DAT levels (47, 48, 62) which is thought to serve as a
545 compensatory adaptation to DAT blockade after repeated cocaine exposure. We hypothesized that
546 ZnT3 KO mice, which lack cocaine-induced Zn^{2+} release and expression of cocaine-induced

547 locomotor sensitization, would be insensitive to cocaine-induced increases in striatal DAT. To test
548 this, mice from the above sensitization experiments were killed 24 hours after the last cocaine
549 injection, the striatum was dissected, and DAT binding assays were performed using [^{3}H]WIN-
550 35,428 (3 repetitions per curve, in triplicate) (one-way ANOVA: $F(3, 8)=6.23$; $p=0.01$). Pairwise
551 comparisons (Holm-Sidak) showed that vehicle-treated WT mice (n=6) did not differ from
552 vehicle- or cocaine-treated ZnT3 KO mice (n=6) in [^{3}H]WIN-35,428 binding (Figure 4D).
553 However, cocaine-treated WT mice (n=6) showed a trend toward greater [^{3}H]WIN-35,428 binding
554 ($t=2.21$; $p=0.058$) compared to vehicle-treated WT mice (n=6) and significantly greater [^{3}H]WIN-
555 35,428 binding than both vehicle-treated (n=6) ($t=4.14$; $p=0.009$) and cocaine-treated KO mice
556 (n=6) ($t=3.12$; $p=0.02$).

557 Next, we tested whether synaptic Zn^{2+} release is involved in cocaine reward by assessing
558 the extent to which ZnT3 KO mice develop cocaine conditioned place preference (CPP). As
559 expected, we found that WT mice showed significant preference for a chamber paired with cocaine
560 (one sample Wilcoxon (non-parametric) test with theoretical median set to 0) at 5 (n=8) ($p=0.007$;
561 95% CI: 41.3 to 336.1), 10 (n=9) ($p=0.003$; 95% CI: 59.2 to 297.3), and 20 (n=8) ($p=0.01$; 95%
562 CI: -9.8 to 258.4) mg/kg. In contrast, ZnT3 KO mice did not show significant preference for the
563 chamber paired with cocaine at any dose: 5 mg/kg (n=7) ($p=0.21$; 95% CI: -118.8 to 256.2), 10
564 mg/kg (n=9) ($p=0.07$; 95% CI: -47.2 to 208.5) and 20 mg/kg (n=7) ($p=0.10$; 95% CI: -140.6 to
565 159.3) (Figure 4E).

566 Finally, we examined whether synaptic Zn^{2+} is involved in intravenous cocaine self-
567 administration (SA). WT mice (n=9) showed robust acquisition of cocaine SA (1 mg/kg/infusion
568 for 13 days), as evidenced by significantly greater (Mixed effects anova with Holm-Sidak multiple
569 comparisons); genotype x session interaction, $F(12, 190)=6.12$; $p<0.001$) and sustained responding
570 on the cocaine-reinforced active lever over the non-reinforced inactive lever on days 11 and 12
571 (session 11: $t=6.48$; $p<0.001$, session 12: $t=4.25$; $p=0.009$) (Figure 4F). In contrast, ZnT3 KO mice
572 (n=9) failed to acquire cocaine SA at the 1 mg/kg/infusion dose (Figure 4H) as they did not show
573 any significant differences (2-way RM anova with Holm-Sidak multiple comparisons, genotype x
574 session interaction, $F(12, 192)=1.27$; $p=0.23$) in cocaine-reinforced vs. inactive lever pressing. All
575 mice were then switched to a lower cocaine dose (0.5 mg/kg/infusion for 7 days). WT mice (n=7)
576 immediately reached the maximum allowed number (50) of infusions (Figure 4G) and showed
577 significantly greater cocaine-reinforced presses (2-way RM anova with Holm-Sidak multiple

comparisons, lever main effect, $F(1, 12)=116.7$; $p<0.001$) compared to inactive lever presses (session 1: $t=12.54$; $p<0.001$, session 2: $t=5.03$; $p=0.004$, session 3: $t=7.91$; $p<0.001$, session 4: $t=9.39$; $p<0.001$, session 5: $t=15.45$; $p<0.001$, session 6: $t=23.33$; $p<0.001$, session 7: $t=10.42$; $p<0.001$). At the 0.5 mg/kg/infusion dose, ZnT3 KO mice took longer (3 sessions) to learn to discriminate the cocaine-reinforced active lever over the inactive lever and also took longer (5 sessions) to reach 50 infusions (Figure 4I). Eventually, ZnT3 KO mice (n=7) showed significantly greater cocaine-reinforced presses (2-way RM anova with Holm-Sidak multiple comparisons, lever x time interaction, $F(6, 71)=3.9$; $p=0.002$) compared to inactive lever presses (session 3: $t=4.74$; $p=0.007$, session 4: $t=7.03$; $p=0.002$, session 5: $t=8.86$; $p<0.001$, session 6: $t=9.82$; $p<0.001$, session 7: $t=4.01$; $p=0.04$). After acquisition of cocaine self-administration, mice were tested at lower doses of cocaine. WT and KO mice did not differ in the number of cocaine infusions at these lower doses (Figure S8). However, compared to WT mice (n=6), KO mice (n=5) showed significantly lower cocaine intake (mixed effects RM analysis with Holm-Sidak multiple comparisons, genotype x dose interaction, $F(4, 44) =2.92$) at 1 mg/kg/inf. ($t=3.26$; $p=0.001$) and at 0.125 mg/kg/inf. ($t=2.03$; $p=0.04$) doses (Figure 4J). Mice were then assessed for extinction of cocaine self-administration, but no genotype differences were observed (Figure 4K). After mice had extinguished their lever responding for cocaine, they were tested for reinstatement (relapse) responding to a cocaine priming injection (10 mg/kg, IP). WT mice (n=5) showed reinstatement of cocaine self-administration and significantly greater active lever presses (2-way RM anova with Holm-Sidak multiple comparisons, genotype x dose interaction, $F(1, 10)=5.09$; $p=0.04$) after cocaine priming ($t=3.17$; $p=0.005$) compared to ZnT3 KO mice (n=5), which did not reinstate (Figure 4L and M). WT mice (n=5) and ZnT3 KO mice (n=5) did not differ in inactive lever responding (2-way RM anova with Holm-Sidak multiple comparisons, genotype x dose interaction, $F(1, 10)=0.17$; $p=0.68$) during cocaine-primed reinstatement.

Dietary Zn^{2+} deficiency decreases brain Zn^{2+} and attenuates cocaine locomotor sensitization, reward, and striatal DAT binding

Synaptic Zn^{2+} levels and ZnT3 expression are modulated by dietary Zn^{2+} intake (30, 31). Chronic drug abuse (including cocaine) in humans is associated with malnutrition and dysregulated peripheral Zn^{2+} levels (33-38). However, whether dietary Zn^{2+} availability can modulate the behavioral effects of cocaine has not been previously reported.

609 To examine this, we fed mice, for approximately one month, diets that were custom-
610 formulated by a commercial vendor to contain either 30 (considered an adequate level of Zn^{2+}
611 intake) or 5 (a low amount of Zn^{2+} intake) ppm Zn^{2+}. We first verified the Zn^{2+} content of each
612 diet using TXRF. According to our measurements, the 30 ppm diet contained ~28 ppm Zn^{2+} and
613 the 5 ppm diet contained ~8 ppm Zn^{2+} (Figure 5A) (we will however refer to them here as 30 and
614 5 ppm Zn^{2+} diets to remain consistent with prior studies that have used similar formulations). Mice
615 fed a 5 ppm Zn^{2+} diet (n=32) did not differ in body weight from mice fed a 30 ppm Zn^{2+} diet (n=32)
616 (Figure 5B). Mice fed a 5 ppm Zn^{2+} diet (n=32) showed a significant decrease (2-way RM anova
617 with Holm-Sidak multiple comparisons; genotype x time interaction, $F(15, 930)=10.07$; $p<0.001$)
618 in food intake 3 days ($t=11.37$; $p<0.001$) after diet initiation compared to mice fed a 30 ppm diet
619 (n=32) though soon afterwards normalized to the same levels of intake (Figure 5C). The low Zn^{2+}
620 diet was effective in decreasing brain Zn^{2+} content as mice fed a 5 ppm Zn^{2+} diet (n=7) showed
621 significantly lower Zn^{2+} levels in frontal cortex (unpaired t-test; $t=3.15$; $p=0.01$) compared to mice
622 fed a 30 pm Zn^{2+} diet (n=5) as assessed via TXRF (Figure 5D).
623 Next, we performed cocaine locomotor sensitization in 30 ppm and 5 ppm mice using the
624 same procedures as in the above ZnT3 KO experiments. Mice fed 5 ppm or 30 ppm Zn^{2+} diets did
625 not differ in the development of cocaine locomotor sensitization (Figure 5E). 30 ppm diet-fed mice
626 injected with cocaine (n=14) showed significantly greater locomotor activity (2-way RM anova
627 with Holm-Sidak multiple comparisons; genotype x session interaction, $F(3, 52)=23.57$; $p<0.001$)
628 than 30 ppm diet-fed mice injected with vehicle (n=14) at Day 1 ($t=8.29$; $p<0.001$) and Day 5
629 ($t=14.27$; $p<0.001$). Similarly, 5 ppm mice injected with cocaine (n=14) showed significantly
630 greater locomotor activity compared to 5 ppm mice injected with vehicle (n=14) at Day 1 ($t=6.95$;
631 $p<0.001$) and Day 5 ($t=13.95$; $p<0.001$). 30 ppm mice injected with cocaine also showed
632 significantly greater locomotor activity at Day 5 than at Day 1 ($t=9.98$; $p<0.001$) and 5 ppm mice
633 injected with cocaine also showed significantly greater locomotor activity at Day 5 than at Day 1
634 ($t=10.06$; $p<0.001$) (Figure 5E). Seven days later, mice were examined for expression of cocaine
635 locomotor sensitization. We found that cocaine-treated mice fed the 30 ppm diet (n=6) showed
636 significantly greater expression of cocaine locomotor sensitization (2-way RM anova with Holm-
637 Sidak multiple comparisons; genotype x time interaction, $F(79, 790)=3.98$; $p<0.001$) at 5 (66 min;
638 $t=5.69$; $p<0.001$, 69 min; $t=4.68$; $p<0.001$, 72 min; $t=3.76$; $p=0.01$, 75 min; $t=3.78$; $p=0.01$, 78
639 min; $t=4.29$; $p=0.001$, 81 min; $t=3.79$; $p=0.01$, 84 min; $t=4.23$; $p=0.002$), 10 mg/kg (123 min;

640 t=5.37; p<0.001, 126 min; t=7.42; p<0.001, 129 min; t=6.99; p<0.001, 132 min; t=6.58; p=0.01,
641 135 min; t=5.08; p=0.03, 138 min; t=5.36; p=0.03, 141 min; t=4.39; p=0.03, 144 min; t=4.14;
642 p=0.03, 147 min; t=3.78; p=0.03) and 20 mg/kg cocaine (183 min; t=3.43; p=0.04) compared to
643 vehicle-treated mice fed the same 30 ppm diet (n=13) (Figure 5F). In contrast, cocaine-treated
644 mice fed the 5 ppm diet (n=6) did not show a significant difference in expression of locomotor
645 sensitization compared to vehicle-treated mice fed the 5 ppm diet (n=6) (2-way RM anova with
646 Holm-Sidak multiple comparisons; genotype x time interaction, F(79, 790)=0.9342; p=0.64)
647 (Figure 5G).

648 Next, we tested whether mice fed 30 ppm and 5 ppm Zn^{2+} diets differed in cocaine
649 preference using the same CPP procedure as in ZnT3 KO mice. Mice fed the 30 ppm Zn^{2+} diet
650 showed significant preference (one sample Wilcoxon test with theoretical median set to 0) for the
651 chamber paired with cocaine at 5 mg/kg (n=8) (p=0.007; 95% CI: 45.8 to 205.5), 10 mg/kg (n=8)
652 (p=0.007; 95% CI: 42.6 to 245.4), and 20 mg/kg (n=7) (p=0.003; 95% CI: -6.0 to 149.6). Mice fed
653 a 5 ppm Zn^{2+} diet showed significant preference (one sample Wilcoxon test with theoretical
654 median set to 0) for the chamber paired with cocaine at 10 mg/kg (n=8) (p=0.039; 95% CI: -79.8
655 to 298.0), and 20 mg/kg (n=8) (p=0.007; 95% CI: 26.2 to 185.9) but not at 5 mg/kg (n=8) (p=0.10;
656 95% CI: -30.1 to 125.7) (Figure 5H).

657 Finally, we examined whether dietary Zn^{2+} availability had any effects on DAT binding in
658 the striatum. Mice fed 30 ppm and 5 ppm Zn^{2+} diets and exposed to escalating cocaine injections
659 (5, 10, and 20 mg/kg, IP, one injection/hour) were killed 24 hours after the last injection and their
660 brains were assessed for striatal [^{3}H]WIN-35,428 binding. We found that mice exposed to cocaine
661 and a 5 ppm Zn^{2+} diet (n=6) showed significantly lower striatal DAT binding (Figure 5I) (unpaired
662 t-test; t=9.63; p<0.001) (3 repetitions per group, in triplicate) and a decrease in cocaine affinity
663 compared to mice exposed to cocaine and a 30 ppm Zn^{2+} diet (n=6) (5ppm K_i=61 ± 26 nM; 30
664 ppm Ki=46 ± 17 nM) (3 repetitions per curve, in triplicate) (Figure 5J).

665

666 **Discussion**

667

668 Here we show that human subjects who died of cocaine overdose had significantly lower
669 Zn^{2+} content in the striatum (caudate) compared to matched controls. We also show that striatal

670 Zn^{2+} levels in these subjects negatively correlated with plasma levels of benzoylecgonine,
671 indicating that low striatal Zn^{2+} levels were associated with greater cocaine intake.

672 To further explore the relationship between cocaine exposure and striatal Zn^{2+}, we
673 performed studies using mice lacking ZnT3, a neuronal Zn^{2+} transporter necessary for synaptic
674 Zn^{2+} release. We found that repeated cocaine injections increased striatal Zn^{2+} content (in CPu and
675 NAc) in normal mice but not in mice lacking ZnT3, indicating that cocaine exposure increases
676 synaptic Zn^{2+} levels in the striatum via the actions of ZnT3. We also found that repeated cocaine
677 injections increased Zn^{2+} uptake in regions with high synaptic Zn^{2+} and ZnT3 content, including
678 the NAc indicating that cocaine exposure increases synaptic Zn^{2+} turnover/metabolism in these
679 regions.

680 We hypothesized that cocaine-induced increases in synaptic Zn^{2+} release would be relevant
681 to cocaine's *in vivo* actions at the DAT, given the known *in vitro* interactions between Zn^{2+}, DAT,
682 and cocaine. Using *in vitro* assays, we first confirmed that a physiologically-relevant concentration
683 of Zn^{2+} increased the ability of cocaine to bind to DAT. Then, to extend the relevance of this
684 finding to an *in vivo* context, we used *in vivo* FSCV and found that deletion of ZnT3, and hence,
685 loss of synaptic Zn^{2+} release, attenuated cocaine's effects on striatal DA neurotransmission.
686 Consistent with this observation, mice lacking ZnT3 were insensitive to cocaine-induced increases
687 in striatal DAT binding and showed attenuated behavioral responses to cocaine in several
688 procedures such as locomotor sensitization, CPP, and IV self-administration, indicating that
689 synaptic Zn^{2+} promotes cocaine sensitization, reward, and cocaine-seeking behavior.

690 Zn^{2+} is obtained almost exclusively from the diet. Taking our above findings into account,
691 we reasoned that low environmental availability of Zn^{2+} and specifically, reduced dietary Zn^{2+}
692 intake, would attenuate behavioral responses to cocaine. As predicted, we found that mice exposed
693 to a diet with low Zn^{2+} content showed lower brain Zn^{2+} levels, decreased cocaine-induced
694 increases in striatal DAT binding, and attenuated behavioral responses to cocaine compared to
695 mice fed a diet with adequate Zn^{2+} content. This indicates that low dietary Zn^{2+} intake decreases
696 brain Zn^{2+} levels, and attenuates cocaine locomotor sensitization, cocaine preference, and cocaine-
697 induced increases in striatal DAT.

698 Taken together, our above findings suggest that synaptic Zn^{2+} release in the striatum plays
699 a critical role in cocaine's effects on striatal DA neurotransmission and consequently in the

700 neurobiological and behavioral adaptations associated with cocaine exposure. A summary
701 depicting this proposed mechanism is shown in Figure 6.

702 The results from our experiments in mice suggest that the Zn^{2+} deficits we identified in
703 humans who died from cocaine overdose may arise from a combination of inadequate nutrition
704 (i.e. low dietary Zn^{2+} intake) and increased Zn^{2+} turnover/metabolism brought upon by chronic
705 cocaine use, although we cannot rule out individual or combined contributions of diet, cocaine use,
706 or use of other drugs/substances in these effects. The negative correlation between striatal Zn^{2+}
707 content and plasma benzoylecgonine levels in postmortem human samples, taken together with the
708 rest of our data, may reflect the notion that individuals with inherently low striatal Zn^{2+} levels
709 would be less sensitive to the effects of cocaine and therefore would need to compensate by
710 consuming more of the drug. This would implicate Zn^{2+} as an environmental factor that could
711 influence vulnerability to the effects of cocaine and potentially to the development of cocaine use
712 disorders or addiction.

713 Our results have important implications for both general DA-dependent behaviors and
714 especially for the prevention and treatment of cocaine addiction. Specifically, our findings suggest
715 that dietary Zn^{2+} intake, and potentially, impaired Zn^{2+} absorption or excretion mechanisms, are
716 implicated in cocaine reward, seeking, and relapse. Consequently, we suggest that the Zn^{2+} status
717 of patients with cocaine addiction should be taken into consideration, especially since Zn^{2+}
718 deficiency varies in prevalence across social demographics and is found in higher proportion in
719 developing countries (32).

720 Our findings also expand the current understanding of cocaine's neurobiological effects.
721 DA and glutamate systems converge at the level of the striatum to modulate behaviors that
722 influence cocaine seeking and abuse (46, 63). Synaptic Zn^{2+}, mediated by ZnT3, is packaged along
723 with glutamate in the same synaptic vesicles and is released by glutamatergic terminals in the
724 striatum upon neuronal activation. As such, the cocaine-induced synaptic Zn^{2+} increases we report
725 here would be expected to accompany the well-described increase in synaptic glutamate
726 neurotransmission in the striatum following repeated cocaine exposure (45, 46, 64, 65). Indeed,
727 cocaine-induced increases in synaptic glutamate are thought to result, in part, from reductions in
728 extrasynaptic glutamate arising from decreased cystine-glutamate exchange in response to
729 repeated cocaine use (63, 66). Specifically, cocaine-induced reductions in extrasynaptic glutamate
730 weaken signaling at presynaptic metabotropic glutamate receptors, thereby increasing synaptic

731 glutamate levels (64) and resulting in excitatory synaptic strengthening. This mechanism may
732 underlie the increases in cocaine-induced synaptic Zn^{2+} that we observe.

733 Zn^{2+} binds to NMDA and AMPA receptors (67, 68) and it is likely that, in addition to
734 affecting DA neurotransmission via binding to DAT, cocaine-induced increases in synaptic Zn^{2+}
735 release may also exert direct allosteric interactions at ionotropic glutamate receptors to influence
736 cocaine-dependent glutamate neurotransmission, synaptic plasticity, and behaviors such as
737 cocaine locomotor sensitization and cocaine priming-induced reinstatement of cocaine seeking
738 (45, 46, 65, 69). However, the precise mechanism for how cocaine-induced Zn^{2+} release would
739 lead to such effects is complicated by the fact that Zn^{2+} can exert bidirectional effects at AMPA
740 receptors (70), it can inhibit both synaptic and extrasynaptic NMDA receptors (68), and finally,
741 that cocaine induces projection- and cell type-specific adaptations in the NAc (71), that not all
742 NAc glutamatergic synapses release Zn^{2+}, and that the specific zincergic synapses, and the
743 postsynaptic cells they target in regions such as the NAc have not yet been defined. For all these
744 reasons, the specific effects of cocaine-induced Zn^{2+} release on glutamatergic signaling are unclear
745 and require further investigation.

746 Another possibility may be that Zn^{2+} interacts with cystine-glutamate exchange
747 mechanisms directly to produce changes in cocaine behaviors. Indeed, we found here that ZnT3
748 KO mice failed to reinstate cocaine-primed self-administration of cocaine, suggesting that synaptic
749 Zn^{2+} release is necessary for cocaine-primed seeking. N-acetylcysteine (NAC) is a derivative of
750 the amino acid cysteine and has been proposed as a treatment for substance use disorders (72).
751 NAC prevents cocaine-primed reinstatement of drug seeking after cocaine self-administration by
752 stimulating cystine-glutamate exchange (63). Importantly, NAC also has metal-chelating
753 capabilities (Zn^{2+} binds with high affinity to cysteines (73)) and systemic administration of NAC
754 in mice has been shown to decrease peripheral Zn^{2+} levels (74). Accordingly, it may be possible
755 that in addition to the effects of NAC in decreasing cocaine-primed seeking via activation of
756 cystine-glutamate exchange, its effects may also be driven, in part, via direct interaction with
757 synaptic Zn^{2+}. In this case, NAC would effectively act as a Zn^{2+} chelating agent, decreasing
758 synaptic Zn^{2+} levels, which would attenuate cocaine's effects at the DAT and decrease cocaine-
759 seeking. However, this could also occur concomitantly to NAC's activation of cystine-glutamate
760 exchange, which would increase extrasynaptic glutamate to restore presynaptic metabotropic
761 glutamate receptor tone and thereby reduce synaptic glutamate and potentially, co-released Zn^{2+}.

762 In addition to cocaine, other psychostimulants interact with the DAT to produce their
763 effects of behavior. We propose that the cocaine-dependent changes in Zn^{2+} that we describe here
764 are not specific to cocaine but may also be elicited by other psychostimulants that modulate DAT
765 function and increase corticostriatal glutamate neurotransmission (45, 46, 75), and potentially
766 other drugs of abuse, including alcohol (76) which is strongly associated with Zn^{2+} deficiency (76).
767 Finally, in addition to its critical role in addiction, the DAT is the primary molecular target
768 for stimulant medications used in the treatment of attention-deficit hyperactivity disorder (ADHD).
769 Studies indicate that medication response is reduced in Zn^{2+}-deficient ADHD patients (77). Our
770 findings here offer a mechanistic explanation for these clinical observations and suggest that Zn^{2+}
771 supplementation may improve the efficacy of stimulant-based ADHD medications.
772 In conclusion, our findings expand current knowledge regarding the direct
773 pharmacological mechanism of action of cocaine and the neurobiological mechanisms involved in
774 cocaine's behavioral effects by identifying a critical role for the trace element Zn^{2+} as an
775 environmentally derived modulator of cocaine affinity, potency, plasticity, reward, and seeking.

Acknowledgments and Author contributions

JLG, JB, SL, DM, KW, MLC, LAR, RJE, CJ, GB, JK, MP, MB, ZX, GT, OS, and MM designed and/or performed experiments and/or analyzed data. ZX, GT, and MM supervised work. JLG, JB, and MM wrote the paper with input from all coauthors. The authors thank Dr. Thanos Tzounopoulos (University of Pittsburgh) for sharing ZnT3 knockout mice, Dr Richard Dyck (University of Calgary) for advice regarding Zn^{2+} staining, Dr. Yavin Shaham (NIDA) for experimental advice in behavioral experimentation and for manuscript comments, and Dr. Marisela Morales (NIDA), Dr. Antonio Lanzirotti, Dr. Keith Jones and William Rao at the National Synchrotron Light Source (NSLS) X26a Beamline at Brookhaven National Laboratory for instrumentation access. This work was supported by the NIDA Intramural Research Program (DA000069), the NIDA Medication Development Program (DA000611) and the Department of Energy (DOE) GeoSciences grant DE-FG02-92ER14244.

Conflict of Interest: The authors have declared that no conflict of interest exists.

References

1. Frederickson CJ, Suh SW, Silva D, and Thompson RB. Importance of zinc in the central nervous system: the zinc-containing neuron. *J Nutr.* 2000;130(5S Suppl):1471s-83s.
2. Gower-Winter SD, and Levenson CW. Zinc in the central nervous system: From molecules to behavior. *Biofactors.* 2012;38(3):186-93.
3. Pfeiffer CC, and Braverman ER. Zinc, the brain and behavior. *Biol Psychiatry.* 1982;17(4):513-32.
4. Sensi SL, Paoletti P, Koh JY, Aizenman E, Bush AI, and Hershfinkel M. The neurophysiology and pathology of brain zinc. *J Neurosci.* 2011;31(45):16076-85.
5. Cuajungco MP, and Lees GJ. Zinc metabolism in the brain: relevance to human neurodegenerative disorders. *Neurobiol Dis.* 1997;4(3-4):137-69.
6. McAllister BB, and Dyck RH. Zinc transporter 3 (ZnT3) and vesicular zinc in central nervous system function. *Neurosci Biobehav Rev.* 2017;80:329-50.
7. Pe´rez-Clausell J, and Danscher G. Intravesicular localization of zinc in rat telencephalic boutons. A histochemical study. *Brain Research.* 1985;337(1):91-8.
8. Brown CE, and Dyck RH. Distribution of zincergic neurons in the mouse forebrain. *Journal of Comparative Neurology.* 2004;479(2):156-67.
9. Palmiter RD, Cole TB, Quaife CJ, and Findley SD. ZnT-3, a putative transporter of zinc into synaptic vesicles. *Proc Natl Acad Sci U S A.* 1996;93(25):14934-9.
10. Cole TB, Wenzel HJ, Kafer KE, Schwartzkroin PA, and Palmiter RD. Elimination of zinc from synaptic vesicles in the intact mouse brain by disruption of the ZnT3 gene. *Proc Natl Acad Sci U S A.* 1999;96(4):1716-21.
11. Thackray SE, McAllister BB, and Dyck RH. Behavioral characterization of female zinc transporter 3 (ZnT3) knockout mice. *Behav Brain Res.* 2017;321:36-49.
12. Cole TB, Martyanova A, and Palmiter RD. Removing zinc from synaptic vesicles does not impair spatial learning, memory, or sensorimotor functions in the mouse. *Brain Res.* 2001;891(1-2):253-65.
13. Martel G, Hevi C, Friebely O, Baybutt T, and Shumyatsky GP. Zinc transporter 3 is involved in learned fear and extinction, but not in innate fear. *Learn Mem.* 2010;17(11):582-90.
14. Kumar M, Xiong S, Tzounopoulos T, and Anderson CT. Fine Control of Sound Frequency Tuning and Frequency Discrimination Acuity by Synaptic Zinc Signaling in Mouse Auditory Cortex. *J Neurosci.* 2019;39(5):854-65.
15. Patrick Wu HP, and Dyck RH. Signaling by Synaptic Zinc is Required for Whisker-Mediated, Fine Texture Discrimination. *Neuroscience.* 2018;369:242-7.
16. Frederickson CJ, Giblin LJ, Krężel A, McAdoo DJ, Muelle RN, Zeng Y, et al. Concentrations of extracellular free zinc (pZn)e in the central nervous system during simple anesthetization, ischemia and reperfusion. *Experimental Neurology.* 2006;198(2):285-93.
17. Frederickson CJ, Giblin LJ, Rengarajan B, Masalha R, Frederickson CJ, Zeng Y, et al. Synaptic release of zinc from brain slices: Factors governing release, imaging, and accurate calculation of concentration. *Journal of Neuroscience Methods.* 2006;154(1):19-29.

835 18. Wu Q, Coffey LL, and Reith ME. Cations affect [3H]mazindol and [3H]WIN 35,428
836 binding to the human dopamine transporter in a similar fashion. *J Neurochem.*
837 1997;69(3):1106-18.
838 19. Scholze P, Norregaard L, Singer EA, Freissmuth M, Gether U, and Sitte HH. The role of
839 zinc ions in reverse transport mediated by monoamine transporters. *J Biol Chem.*
840 2002;277(24):21505-13.
841 20. Liang YJ, Zhen J, Chen N, and Reith ME. Interaction of catechol and non-catechol
842 substrates with externally or internally facing dopamine transporters. *J Neurochem.*
843 2009;109(4):981-94.
844 21. Hong WC, and Amara SG. Membrane cholesterol modulates the outward facing
845 conformation of the dopamine transporter and alters cocaine binding. *J Biol Chem.*
846 2010;285(42):32616-26.
847 22. Norregaard L, Frederiksen D, Nielsen EO, and Gether U. Delineation of an endogenous
848 zinc-binding site in the human dopamine transporter. *Embo j.* 1998;17(15):4266-73.
849 23. Kuhar MJ, Ritz MC, and Boja JW. The dopamine hypothesis of the reinforcing properties
850 of cocaine. *Trends Neurosci.* 1991;14(7):299-302.
851 24. Volkow ND, Wang GJ, Fischman MW, Foltin RW, Fowler JS, Abumrad NN, et al.
852 Relationship between subjective effects of cocaine and dopamine transporter occupancy.
853 *Nature.* 1997;386(6627):827-30.
854 25. Wise RA, and Bozarth MA. A psychomotor stimulant theory of addiction. *Psychol Rev.*
855 1987;94(4):469-92.
856 26. Mengual E, Casanovas-Aguilar C, Pérez-Clausell J, and Giménez-Amaya JM.
857 Heterogeneous and compartmental distribution of zinc in the striatum and globus pallidus
858 of the rat. *Neuroscience.* 1995;66(3):523-37.
859 27. Frederickson CJ, Rampy BA, Reamy-Rampy S, and Howell GA. Distribution of
860 histochemically reactive zinc in the forebrain of the rat. *Journal of Chemical*
861 *Neuroanatomy.* 1992;5(6):521-30.
862 28. Ciliax BJ, Drash GW, Staley JK, Haber S, Mobley CJ, Miller GW, et al.
863 Immunocytochemical localization of the dopamine transporter in human brain. *J Comp*
864 *Neurol.* 1999;409(1):38-56.
865 29. Sikora J, Kieffer BL, Paoletti P, and Ouagazzal AM. Synaptic zinc contributes to motor
866 and cognitive deficits in 6-hydroxydopamine mouse models of Parkinson's disease.
867 *Neurobiol Dis.* 2020;134:104681.
868 30. Grabrucker S, Jannetti L, Eckert M, Gaub S, Chhabra R, Pfaender S, et al. Zinc
869 deficiency dysregulates the synaptic ProSAP/Shank scaffold and might contribute to
870 autism spectrum disorders. *Brain.* 2013;137(1):137-52.
871 31. Takeda A, Hirate M, Tamano H, Nisibaba D, and Oku N. Susceptibility to kainate-
872 induced seizures under dietary zinc deficiency. *J Neurochem.* 2003;85(6):1575-80.
873 32. Prasad AS. Discovery of human zinc deficiency: its impact on human health and disease.
874 *Adv Nutr.* 2013;4(2):176-90.
875 33. Santolaria-Fernandez FJ, Gomez-Sirvent JL, Gonzalez-Reimers CE, Batista-Lopez JN,
876 Jorge-Hernandez JA, Rodriguez-Moreno F, et al. Nutritional assessment of drug addicts.
877 *Drug Alcohol Depend.* 1995;38(1):11-8.
878 34. Comai S, Bertazzo A, Vachon J, Daigle M, Toupin J, Cote G, et al. Trace elements
879 among a sample of prisoners with mental and personality disorders and aggression:
880 correlation with impulsivity and ADHD indices. *J Trace Elem Med Biol.* 2019;51:123-9.

881 35. Sadlik J, Pach J, Winnik L, and Piekoszewski W. [Concentration of zinc, copper and
882 magnesium in the serum of drug addicts]. *Przegl Lek.* 2000;57(10):563-4.
883 36. Cheng FL, Wang H, Wu J, Ning MX, Hu LF, and Su YL. [Determination and correlation
884 analysis of trace elements in hair of dependence drug addicts]. *Guang Pu Xue Yu Guang*
885 *Pu Fen Xi.* 2005;25(1):116-8.
886 37. Ruiz Martinez M, Gil Extremera B, Maldonado Martin A, Cantero-Hinojosa J, and
887 Moreno-Abadia V. Trace elements in drug addicts. *Klin Wochenschr.* 1990;68(10):507-
888 11.
889 38. Hossain KJ, Kamal MM, Ahsan M, and Islam SN. *Subst Abuse Treat Prev Policy*.
890 2007:12.
891 39. Bannon MJ, Johnson MM, Michelhaugh SK, Hartley ZJ, Halter SD, David JA, et al. A
892 molecular profile of cocaine abuse includes the differential expression of genes that
893 regulate transcription, chromatin, and dopamine cell phenotype.
894 *Neuropsychopharmacology.* 2014;39(9):2191-9.
895 40. Zhou Y, Michelhaugh SK, Schmidt CJ, Liu JS, Bannon MJ, and Lin Z. Ventral midbrain
896 correlation between genetic variation and expression of the dopamine transporter gene in
897 cocaine-abusing versus non-abusing subjects. *Addict Biol.* 2014;19(1):122-31.
898 41. Stan AD, Ghose S, Gao XM, Roberts RC, Lewis-Amezcua K, Hatanpaa KJ, et al. Human
899 postmortem tissue: what quality markers matter? *Brain Res.* 2006;1123(1):1-11.
900 42. Michaelides M, Pascau J, Gispert JD, Delis F, Grandy DK, Wang GJ, et al. Dopamine D4
901 receptors modulate brain metabolic activity in the prefrontal cortex and cerebellum at rest
902 and in response to methylphenidate. *Eur J Neurosci.* 2010;32(4):668-76.
903 43. Keighron JD, Quarterman JC, Cao J, DeMarco EM, Coggiano MA, Gleaves A, et al.
904 Effects of (R)-Modafinil and Modafinil Analogues on Dopamine Dynamics Assessed by
905 Voltammetry and Microdialysis in the Mouse Nucleus Accumbens Shell. *ACS Chem*
906 *Neurosci.* 2019;10(4):2012-21.
907 44. Ho J, Tumkaya T, Aryal S, Choi H, and Claridge-Chang A. Moving beyond P values:
908 data analysis with estimation graphics. *Nature Methods.* 2019;16(7):565-6.
909 45. Scofield MD, Heinsbroek JA, Gipson CD, Kupchik YM, Spencer S, Smith AC, et al. The
910 Nucleus Accumbens: Mechanisms of Addiction across Drug Classes Reflect the
911 Importance of Glutamate Homeostasis. *Pharmacol Rev.* 2016;68(3):816-71.
912 46. Schmidt HD, and Pierce RC. Cocaine-induced neuroadaptations in glutamate
913 transmission: Potential therapeutic targets for craving and addiction. *Ann N Y Acad Sci.*
914 2010;1187:35-75.
915 47. Proebstl L, Kamp F, Manz K, Krause D, Adorjan K, Pogarell O, et al. Effects of
916 stimulant drug use on the dopaminergic system: A systematic review and meta-analysis
917 of in vivo neuroimaging studies. *Eur Psychiatry.* 2019;59:15-24.
918 48. Little KY, Zhang L, Desmond T, Frey KA, Dalack GW, and Cassin BJ. Striatal
919 dopaminergic abnormalities in human cocaine users. *Am J Psychiatry.* 1999;156(2):238-
920 45.
921 49. Jufer RA, Wstadik A, Walsh SL, Levine BS, and Cone EJ. Elimination of cocaine and
922 metabolites in plasma, saliva, and urine following repeated oral administration to human
923 volunteers. *J Anal Toxicol.* 2000;24(7):467-77.
924 50. Qin Z, Caruso JA, Lai B, Matusch A, and Becker JS. Trace metal imaging with high
925 spatial resolution: applications in biomedicine. *Metallomics.* 2011;3(1):28-37.

926 51. Linkous DH, Flinn JM, Koh JY, Lanzirotti A, Bertsch PM, Jones BF, et al. *J Histochem*
927 *Cytochem*. 2008:3-6.
928 52. Danscher G, and Stoltenberg M. Zinc-specific autometallographic in vivo selenium
929 methods: tracing of zinc-enriched (ZEN) terminals, ZEN pathways, and pools of zinc
930 ions in a multitude of other ZEN cells. *J Histochem Cytochem.* 2005;53(2):141-53.
931 53. Sorensen JC, Slomianka L, Christensen J, and Zimmer J. Zinc-containing telencephalic
932 connections to the rat striatum: a combined Fluoro-Gold tracing and histochemical study.
933 *Exp Brain Res.* 1995;105(3):370-82.
934 54. Takeda A, Sawashita J, and Okada S. Biological half-lives of zinc and manganese in rat
935 brain. *Brain Res.* 1995;695(1):53-8.
936 55. Pullen RGL, Franklin PA, and Hall GH. 65Zn Uptake from Blood into Brain in the Rat.
937 *Journal of Neurochemistry.* 1991;56(2):485-9.
938 56. Takeda A, Hirate M, and Oku N. Elimination of zinc-65 from the brain under kainate-
939 induced seizures. *Biometals.* 2004;17(2):141-4.
940 57. Takeda A, Kodama Y, Ohnuma M, and Okada S. Zinc transport from the striatum and
941 substantia nigra. *Brain Res Bull.* 1998;47(1):103-6.
942 58. Takeda A, Minami A, Takefuta S, Tochigi M, and Oku N. Zinc homeostasis in the brain
943 of adult rats fed zinc-deficient diet. *J Neurosci Res.* 2001;63(5):447-52.
944 59. Wang F, Dufner-Beattie J, Kim BE, Petris MJ, Andrews G, and Eide DJ. Zinc-stimulated
945 endocytosis controls activity of the mouse ZIP1 and ZIP3 zinc uptake transporters. *J Biol*
946 *Chem.* 2004;279(23):24631-9.
947 60. Bjorklund NL, Volz TJ, and Schenk JO. Differential effects of Zn2+ on the kinetics and
948 cocaine inhibition of dopamine transport by the human and rat dopamine transporters.
949 *Eur J Pharmacol.* 2007;565(1-3):17-25.
950 61. Pifl C, Wolf A, Rebernik P, Reither H, and Berger ML. Zinc regulates the dopamine
951 transporter in a membrane potential and chloride dependent manner.
952 *Neuropharmacology.* 2009;56(2):531-40.
953 62. Malison RT, Best SE, van Dyck CH, McCance EF, Wallace EA, Laruelle M, et al.
954 Elevated striatal dopamine transporters during acute cocaine abstinence as measured by
955 [123I] beta-CIT SPECT. *Am J Psychiatry.* 1998;155(6):832-4.
956 63. Baker DA, McFarland K, Lake RW, Shen H, Tang XC, Toda S, et al. Neuroadaptations
957 in cystine-glutamate exchange underlie cocaine relapse. *Nat Neurosci.* 2003;6(7):743-9.
958 64. Moran MM, McFarland K, Melendez RI, Kalivas PW, and Seamans JK.
959 Cystine/glutamate exchange regulates metabotropic glutamate receptor presynaptic
960 inhibition of excitatory transmission and vulnerability to cocaine seeking. *J Neurosci.*
961 2005;25(27):6389-93.
962 65. Wolf ME. The Bermuda Triangle of cocaine-induced neuroadaptations. *Trends in*
963 *Neurosciences.* 2010;33(9):391-8.
964 66. Baker DA, Xi Z-X, Shen H, Swanson CJ, and Kalivas PW. The Origin and Neuronal
965 Function of In Vivo Nonsynaptic Glutamate. *The Journal of Neuroscience.*
966 2002;22(20):9134-41.
967 67. Kalappa BI, Anderson CT, Goldberg JM, Lippard SJ, and Tzounopoulos T. AMPA
968 receptor inhibition by synaptically released zinc. *Proc Natl Acad Sci U S A.*
969 2015;112(51):15749-54.

68. Anderson CT, Radford RJ, Zastrow ML, Zhang DY, Apfel UP, Lippard SJ, et al. Modulation of extrasynaptic NMDA receptors by synaptic and tonic zinc. *Proc Natl Acad Sci U S A.* 2015;112(20):E2705-14.
69. Fouyssac M, and Belin D. Beyond drug-induced alteration of glutamate homeostasis, astrocytes may contribute to dopamine-dependent intrastriatal functional shifts that underlie the development of drug addiction: A working hypothesis. *Eur J Neurosci.* 2019;50(6):3014-27.
70. Blakemore LJ, and Trombley PQ. Mechanisms of zinc modulation of olfactory bulb AMPA receptors. *Neuroscience.* 2019;410:160-75.
71. Zinsmaier AK, Dong Y, and Huang YH. Cocaine-induced projection-specific and cell type-specific adaptations in the nucleus accumbens. *Molecular Psychiatry.* 2021.
72. Tomko RL, Jones JL, Gilmore AK, Brady KT, Back SE, and Gray KM. N-acetylcysteine: A potential treatment for substance use disorders. *Curr Psychiatr.* 2018;17(6):30-55.
73. Pace NJ, and Weerapana E. Zinc-binding cysteines: diverse functions and structural motifs. *Biomolecules.* 2014;4(2):419-34.
74. Wolfram T, Schwarz M, Reuß M, Lossow K, Ost M, Klaus S, et al. N-Acetylcysteine as Modulator of the Essential Trace Elements Copper and Zinc. *Antioxidants (Basel).* 2020;9(11):1117.
75. Bonaventura J, Quiroz C, Cai NS, Rubinstein M, Tanda G, and Ferre S. Key role of the dopamine D4 receptor in the modulation of corticostriatal glutamatergic neurotransmission. *Sci Adv.* 2017;3(1):e1601631.
76. Skalny AV, Skalnaya MG, Grabeklis AR, Skalnaya AA, and Tinkov AA. Zinc deficiency as a mediator of toxic effects of alcohol abuse. *Eur J Nutr.* 2018;57(7):2313-22.
77. Lepping P, and Huber M. Role of zinc in the pathogenesis of attention-deficit hyperactivity disorder: implications for research and treatment. *CNS Drugs.* 2010;24(9):721-8.

1016 **Figure 1**

1017

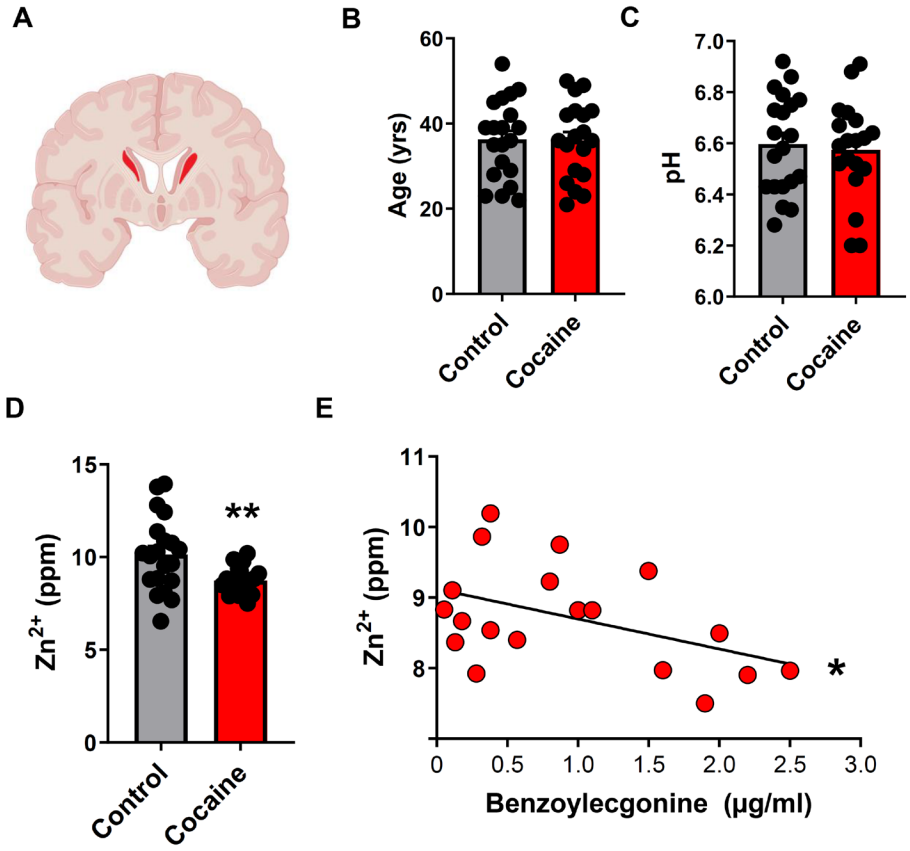

1019 **Striatal Zn^{2+} is low in human cocaine users and correlates with cocaine intake.**
1020 (**A**) Schematic showing sampled region (caudate) from postmortem human brain samples. (**B**)
1021 Cocaine users and control subjects did not differ in age or (**C**) in tissue pH. (**D**) Cocaine users
1022 showed significantly lower striatal Zn^{2+} levels compared to control subjects. (**E**) Striatal Zn^{2+}
1023 levels in cocaine users significantly correlated with plasma benzoylecgonine levels (ppm – parts
1024 per million). **$p \leq 0.01$, *$p \leq 0.05$. All data expressed as Mean ±SEM.

1025

Figure 2

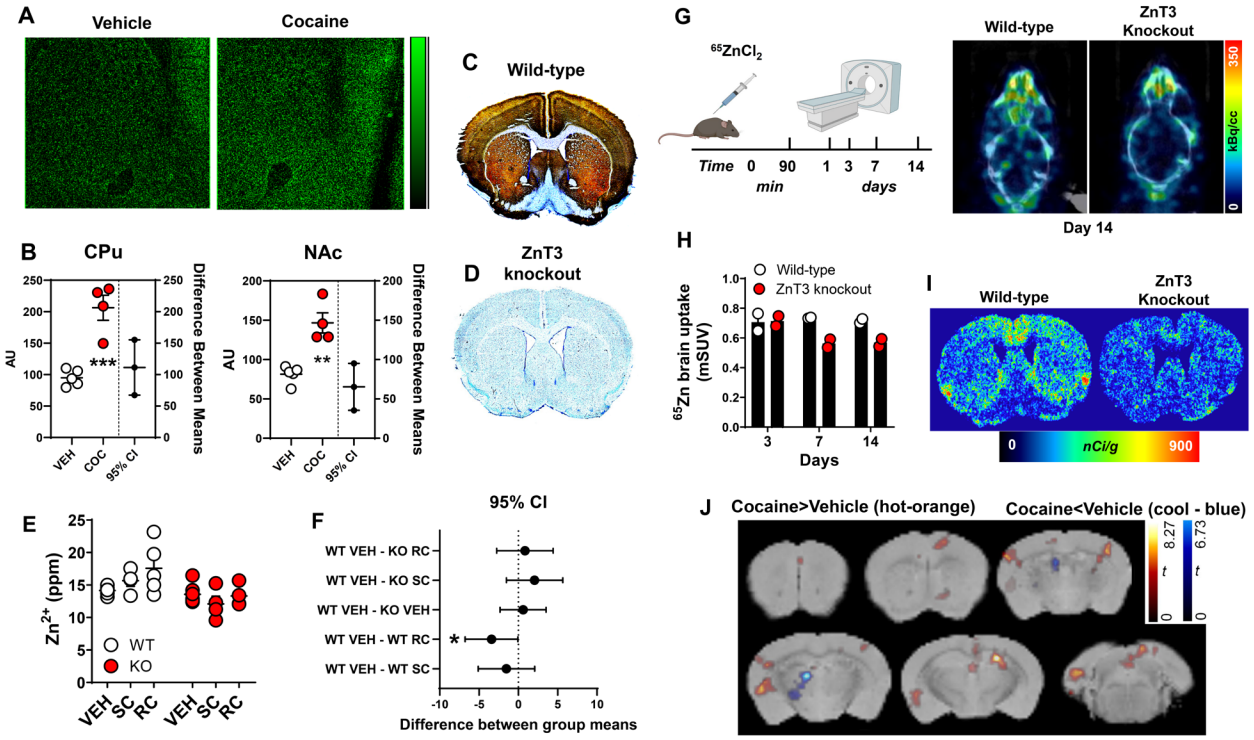

Cocaine increases synaptic Zn^{2+} release and uptake in the striatum. (**A**) Representative synchrotron X-ray fluorescence microspectroscopy (µSXRF) Zn^{2+} maps from vehicle- or cocaine-treated mice. (**B**) Cocaine-treated mice had significantly greater Zn^{2+} (AU-arbitrary units) than vehicle-treated mice in caudate putamen (CPu) and nucleus accumbens (NAc). (**C**) Representative Timm- and cresyl violet- co-stained sections from a wild-type (WT) and (**D**) a ZnT3 knockout (KO) mouse. (**E**) Zn^{2+} content measured using TXRF in wild-type and ZnT3 knockout mice exposed to vehicle (VEH), a single cocaine injection (SC) or repeated cocaine injections (RC) injections. (**F**) Wild-type mice exposed to RC had significantly greater Zn^{2+} levels compared to VEH-treated WT mice. (**G**) PET experimental timeline and representative horizontal ^{65}Zn PET/CT images from wild-type and ZnT3 knockout mice scanned at 14 days after $^{65}ZnCl_2$ administration. (**H**) $^{65}ZnCl_2$ brain uptake expressed as mean standard uptake value (mSUV) in wild-type and knockout mice scanned at 3, 7 and 14 days after injection. (**I**) Representative $^{65}ZnCl_2$ autoradiograms from wild-type and ZnT3 knockout mice scanned using PET at day 15 after $^{65}ZnCl_2$ administration and then killed for postmortem verification. (**J**) Statistical contrasts from voxel-wise statistical parametric mapping analyses from vehicle- or cocaine-treated mice exposed to $^{65}ZnCl_2$ PET imaging. ppm – parts per million. *$p \leq 0.05$, **$p \leq 0.01$, ***$p \leq 0.001$. All data expressed as Mean ±SEM.

1052 **Figure 3**

1053

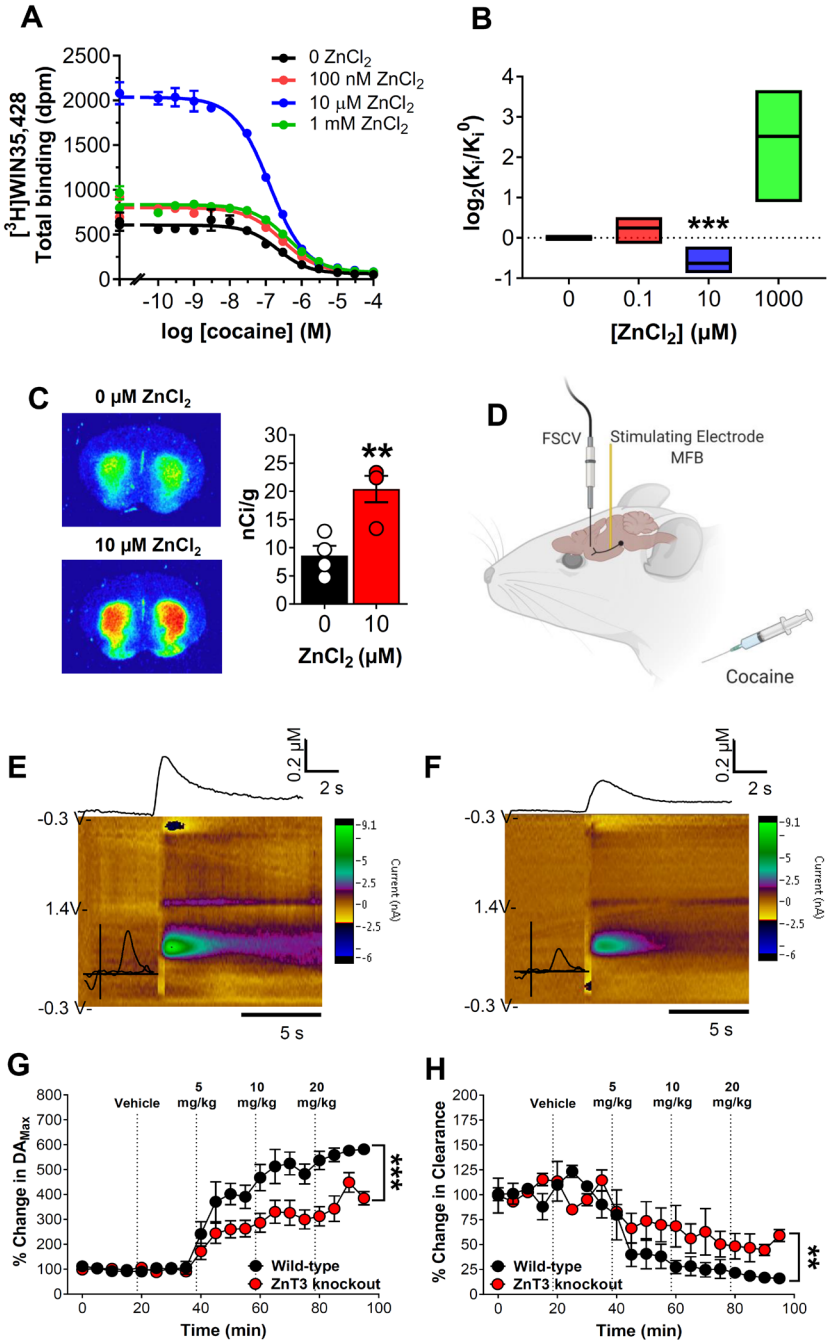

1055 **Synaptic Zn^{2+} release increases the *in vivo* potency of cocaine on striatal DA**
1056 **neurotransmission**. (**A**) Competition binding curves of cocaine and $ZnCl_2$ against [^{3}H]WIN-
1057 35,428 in mouse striatal tissue. (**B**) 10 μM $ZnCl_2$ significantly increased and 1 mM $ZnCl_2$ decreased
1058 affinity of cocaine in mouse striatum (Ki (±SD)) values in nM; Cocaine: 0 μM Zn, 63±39; 0.1 μM
1059 Zn, 77±57; 10 μM Zn, 43±31; 1000 μM Zn, 611±843 and WIN35,428: 0 μM Zn, 9±1.2; 0.1 μM

1060 Zn, 9.2±0.8; 10 μM Zn, 5.1±1.1; 1000 μM Zn, 13.4±1.8). (**C**) Autoradiograms at the level of
1061 mouse striatum showing that 10 μM $ZnCl_2$ significantly increased [^{3}H]WIN-35,428 binding. (**D**)
1062 Experimental design of fast scan cyclic voltammetry (FSCV) experiment. (**E**) Representative
1063 FSCV color plots from wild-type and (**F**) ZnT3 knockout mice showing changes in electrically-
1064 evoked dopamine (DA) after a 10 mg/kg IP cocaine injection. (**G**) FSCV time-course plots
1065 showing significantly lower percent change in electrically-evoked DA_{Max} and (**H**) faster DA
1066 Clearance rate in ZnT3 knockout compared to wild-type mice as a function of vehicle or escalating
1067 IP cocaine injections. *$p \leq 0.05$, **$p \leq 0.01$, ***$p \leq 0.001$. All data expressed as Mean ±SEM.
1068

1069 **Figure 4**

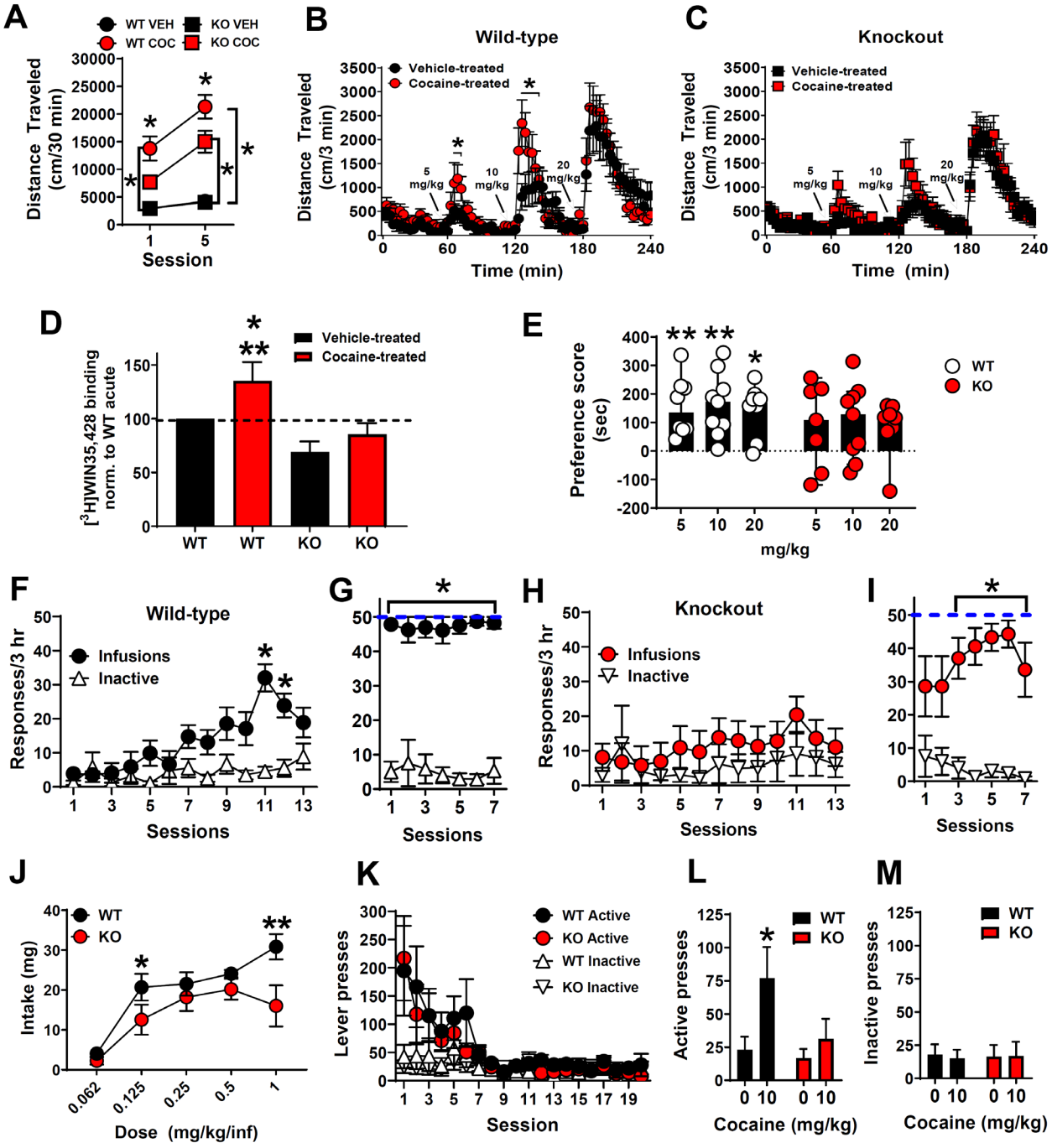

1072

1073 **Synaptic Zn^{2+} release potentiates cocaine locomotor sensitization, reward, seeking and is**

1074 **required for cocaine-induced increases in DAT**

1075 (**A**) ZnT3 knockout (KO) mice injected with 10 mg/kg cocaine (COC) showed significantly lower
1076 locomotor activity compared to cocaine-injected wild-type (WT) mice. Compared to vehicle,
1077 cocaine significantly increased locomotor activity in both WT and KO mice on Day 5 but only in
1078 WT mice on Day 1. (**B**) Cocaine-treated WT mice showed significantly greater expression of
1079 cocaine locomotor sensitization at 5 and 10 mg/kg cocaine compared to vehicle-treated WT mice.
1080 (**C**) Cocaine-treated ZnT3 KO mice do not differ in expression of cocaine locomotor sensitization
1081 compared to vehicle-treated KO mice. (**D**) Cocaine-treated WT mice had significantly greater
1082 DAT binding than cocaine-treated ZnT3 KO mice and vehicle-treated KO mice and showed a
1083 trend toward significantly greater DAT binding than vehicle-treated WT mice. (**E**) WT mice
1084 showed significant preference for a chamber paired with cocaine at 5, 10, and 20 mg/kg. ZnT3 KO
1085 mice did now show preference for a chamber paired with cocaine at any dose. (**F**) Wild-type mice
1086 exposed to a training dose of cocaine (1 mg/kg/inf.) showed significantly greater cocaine-
1087 reinforced presses compared to inactive lever presses. (**G**) Once trained, WT mice were exposed
1088 to a lower cocaine dose (0.5 mg/kg/inf.), immediately reached the maximum number of presses
1089 allowed per session, and showed significantly greater cocaine-reinforced presses compared to
1090 inactive lever presses on all sessions. (**H**) ZnT3 knockout mice exposed to a training dose of
1091 cocaine (1 mg/kg/inf.) did not show any significant differences between cocaine-reinforced and
1092 inactive lever pressing. (**I**) ZnT3 knockout mice exposed to a lower cocaine dose (0.5 mg/kg/inf.)
1093 showed significantly greater cocaine-reinforced presses compared to inactive lever presses during
1094 the last 5 sessions. (**J**) ZnT3 KO mice showed significantly lower cocaine intake at 1 mg/kg/inf.
1095 and at 0.125 mg/kg/inf. compared to WT mice. (**K**) WT and ZnT3 KO mice did not differ in
1096 extinction of cocaine self-administration. (**L**) After extinction of cocaine self-administration
1097 behavior, WT mice showed reinstatement of cocaine self-administration and significantly greater
1098 active lever presses after cocaine priming compared to ZnT3 KO mice. (**N**) WT and ZnT3 KO
1099 mice did not differ in inactive lever responding during cocaine-primed reinstatement. *$p \leq 0.05$. All
1100 data except panel E expressed as Mean ±SEM. Panel E is expressed as Median ±95% CI.
1101

1102 **Figure 5**

1103

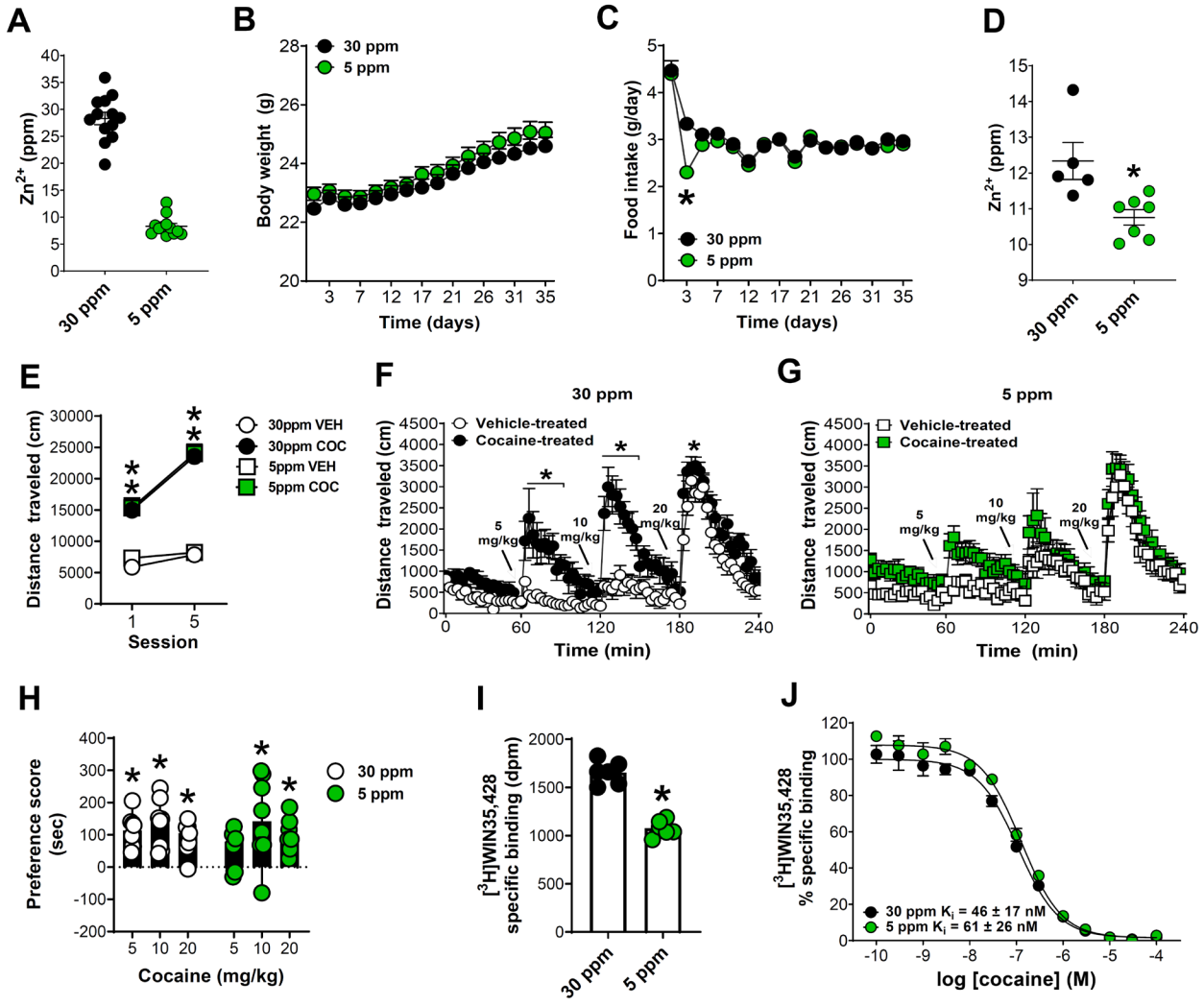

1105

1106 **Dietary Zn^{2+} deficiency decreases brain Zn^{2+} and attenuates cocaine locomotor sensitization,**
1107 **reward and striatal DAT binding.** (**A**) Total reflection X-ray spectroscopy (TXRF)-based
1108 verification of Zn^{2+} content in custom-made diets. (**B**) Mice fed a 5 ppm Zn^{2+} diet did not differ in
1109 body weight from mice fed a 30 ppm Zn^{2+} diet. (**C**) Mice fed a 5 ppm Zn^{2+} diet showed a significant
1110 decrease in food intake 3 days after diet initiation compared to mice fed a 30 ppm diet but did not
1111 differ at other times. (**D**) Mice fed a 5 ppm Zn^{2+} diet showed significantly lower total Zn^{2+} in
1112 frontal/cingulate cortex compared to mice fed a 30 pm Zn^{2+} diet. (**E**) Mice fed 5 ppm or 30 ppm
1113 Zn^{2+} diets did not differ in development of cocaine (COC) locomotor sensitization (VEH- vehicle).
1114 (**F**) Cocaine-treated 30 ppm diet mice (n=6) showed significantly greater expression of cocaine

locomotor sensitization at 5, 10 mg/kg and 20 mg/kg cocaine compared to vehicle-treated 30 ppm mice (n=13). (**G**) Cocaine-treated 5 ppm mice did not show any significant difference in expression of locomotor sensitization compared to vehicle-treated 5 ppm mice. (**H**) Mice fed a 30 ppm Zn^{2+} diet showed significant preference for a chamber paired with cocaine at 5, 10, and 20 mg/kg. Mice fed a 5 ppm Zn^{2+} diet showed significant preference for a chamber paired with cocaine at 10, and 20 mg/kg but not at 5 mg/kg. (**I**) Mice exposed to cocaine and a 5 ppm Zn^{2+} diet showed significantly lower DAT binding in striatum and (**J**) a mild decrease in cocaine affinity compared to mice exposed to cocaine and a 30 ppm diet. dpm - disintegrations per minute. *$p \leq 0.05$. All data except panel H expressed as Mean ±SEM. Panel H is expressed as Median ±95% CI.

1146 Figure 6.

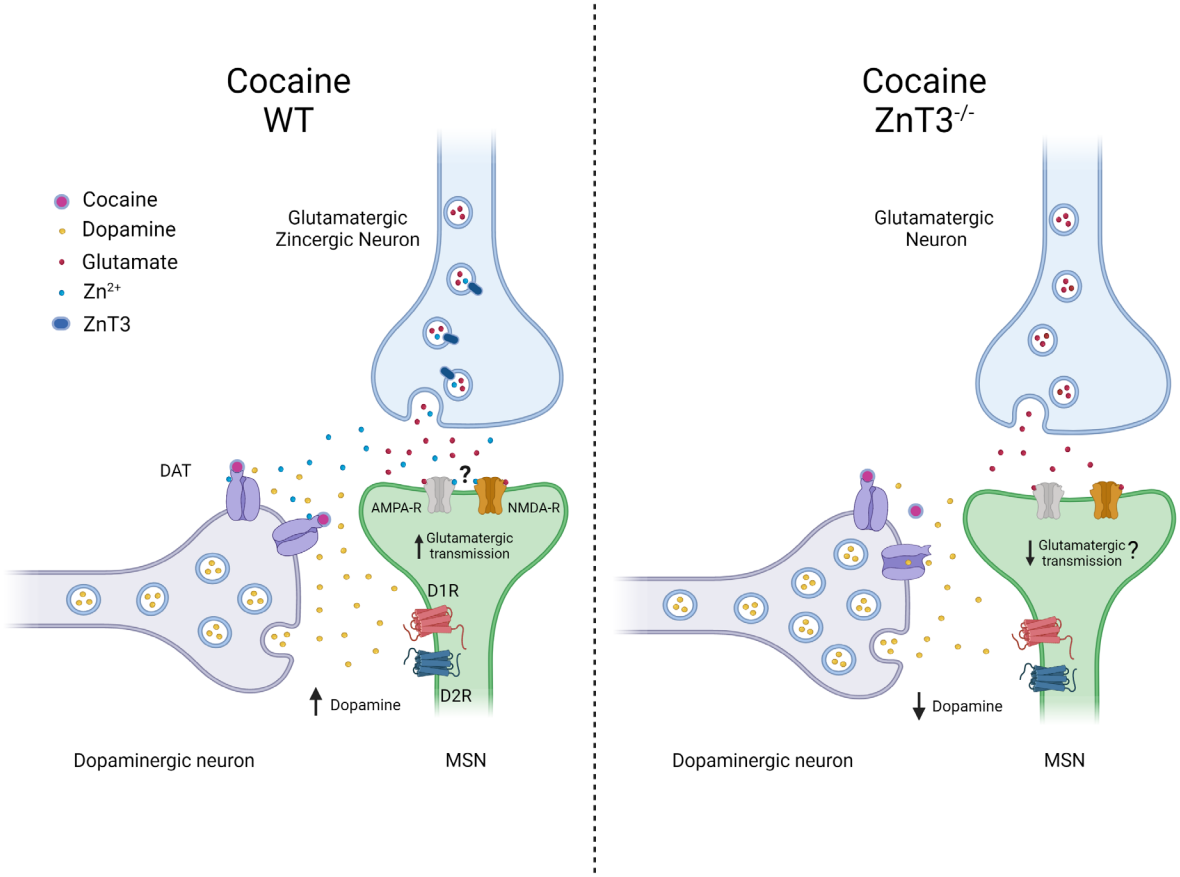

1148 Schematic representation of the putative mechanism by which presynaptic Zn^{2+} modulates the
1149 effects of cocaine on dopamine and glutamate neurotransmission in the striatum in wild-type
1150 (WT) and ZnT3 knockout mice. The image on the left shows the effect of synaptic Zn^{2+} on
1151 increasing cocaine's efficacy by binding to the DAT on dopaminergic neurons. It also
1152 acknowledges the putative effects of Zn^{2+} on glutamate neurotransmission in the context of
1153 cocaine via its interaction with AMPA and NMDA receptors. The image on the right illustrates
1154 the effect of ZnT3 deletion, and consequently the loss of presynaptic Zn^{2+} release, in attenuating
1155 the effects of cocaine on striatal dopamine and glutamate neurotransmission.
1156

1157